Published for SISSA by Springer

Received: June 3, 2019
Revised: August 30, 2019
Accepted: September 29, 2019
Published: October 21, 2019

Low x physics as an infinite twist (G)TMD framework: unravelling the origins of saturation

Tolga Altinoluk[a] **and Renaud Boussarie**[b]

[a] *National Centre for Nuclear Research, 00-681 Warsaw, Poland*
[b] *Physics Department, Brookhaven National Laboratory, Upton, NY 11973, U.S.A.*

E-mail: tolga.altinoluk@ncbj.gov.pl, rboussarie@bnl.gov

Abstract: We show how the formulations of low x physics involving Wilson line operators can be fully rewritten into an infinite twist TMD or GTMD framework, respectively for inclusive and exclusive observables. This leads to a perfect match between low x physics and moderate x formulations of QCD in terms of GTMDs, TMDs, GPDs or PDFs. We derive the BFKL limit as a kinematic limit and argue that beyond the Wandzura-Wilczek approximation, 3-body and 4-body unintegrated PFDs should be taken into account even in this regime. Finally we analyse how saturation should be understood as 3 distinct effects: saturation through non-linearities in the evolution equations at small x, saturation through multiple interactions with slow gluons as TMD gauge links, and saturation as the enhancement of genuine twist corrections.

Keywords: Heavy Ion Phenomenology

ArXiv ePrint: 1902.07930

https://doi.org/10.1007/JHEP10(2019)208

JHEP10(2019)208

Contents

JHEP10(2019)208

1 Introduction

The continuity between moderate x and low x observables has been the subject of many studies in perturbative QCD. The factorization schemes involved in both cases seem indeed very different at first sight. For processes where the center-of-mass energy s is of the same order as the hard partonic scale Q^2, i.e. at moderate $x = Q^2/s$, and for inclusive enough observables, colinear factorization applies. The simplicity of having a single hard scale carried by a single hard momentum allows for a standard Operator Product Expansion (OPE) to be performed. Such an OPE consists in the expansion of a bilocal operator into a discrete set of local operators $\mathcal{O}_n$, usually ordered according to their twist (dimension − spin). For example for quark currents J the OPE has the form:

$$J(z)J(0) \to \sum_n C_n(z,\mu)\,\mathcal{O}_n(\mu)\,, \tag{1.1}$$

where μ is a renormalization scale and where divergences from the loop corrections to the Wilson coefficient $C_n(z,\mu)$ are cancelled via the renormalization of the local operator $\mathcal{O}_n(\mu)$. This renormalization allows to resum large logarithms of the hard scale Q. In the low x limit, the hardest scale of the process is given by s, and the previous OPE is not convenient to address logarithms of this scale. The low x OPE developed in [1–3], to which we will refer as the shockwave framework, has a very different form:

$$J(z)J(0) \to C_0(z,Y_c)\,\mathcal{O}_0(Y_c) + \alpha_s C_1(z,Y_c)\,\mathcal{O}_1(Y_c) + \dots\,, \tag{1.2}$$

where Y_c is a rapidity separation scale and where the spurious rapidity divergence from the 1-loop correction to the C_{n+1} coefficient is cancelled by the Leading Logarithmic (LL) Y_c evolution of the n-th operator $\mathcal{O}_n$, and so on and so forth. Such an evolution in Y_c allows to resum large logarithms of s.

It is possible to take the low x limit in eq. (1.1) and to match it to the first powers of the partonic hard scale in eq. (1.2). However, eq. (1.1) is usually valid for the first few powers at best while eq. (1.2) is valid for all powers of Q. On the flip side so far only the first few subleading $s^{-1/2}$ corrections to eq. (1.2) have been computed [4–13] while eq. (1.1) is valid for all powers of s.

The main difficulty in finding a general continuity between both schemes is the nature of the operators involved. While the moderate x factorization schemes involve operators which consist of parton fields with the appropriate gauge links, the low x schemes involve full Wilson line operators. This difficulty is the one we will address in this article.

For several processes and in several kinematic regimes, a matching between the low x Wilson line operators and some standard moderate x distributions have been found. Transverse Momentum Dependent (TMD) distributions were first recovered in [14, 15] via a so-called *correlation* expansion, which was extended in [16] for 3-particle final states and to infinite kinematic twist accuracy in [17]. The correspondance between low x and TMD observables is the subject of many recent studies [18–23]. For a review on TMD gluon distributions at small x, the reader is referred to [24]. The off-forward generalization of TMD distributions (Generalized TMD distributions, GTMD) and their Fourier transforms, the Wigner distributions, were also found in [25, 26]. Generalized Parton Distributions (GPD), the off-forward extension of PDFs, were extracted via a twist expansion in [27]. In this article, we develop a method to rewrite low x physics in terms of TMD and Wigner distributions, which are known to span PDFs and GPDs as well [28, 29], allowing for a completely systematic rewriting of low x observables in terms the distributions involved in the moderate x regime as well. Our formulation of low x physics is that of an infinite twist (G)TMD framework.

The question of gluon saturation is one of the most exciting topics in low x physics. While the original Balitsky Fadin Kuraev Lipatov (BFKL) description [30, 31] did not involve saturation effects, the more recent dipole [32–34] and shockwave [1–3] frameworks contain non-linear effects embedded in their evolution equation. More strikingly, the effective Feynman rules and Wilson line operators involved in the shockwave framework were shown to be perfectly compatible with earlier results [35–37] describing scattering off a heavy ion with large gluon occupancy taken into account as the very starting point. The low x description of scattering off nuclear targets, known as the Color Glass Condensate (CGC) [38], also has the exact same hierarchy of evolution equations as in [1–3], the Balitsky-Jalilian-Marian-Iancu-McLerran-Weigert-Leonidov-Kovner (B-JIMWLK) evolution equation [39–46], which reduces in the mean field approximation to the Balitsky-Kovchegov (BK) equation, the evolution equation in the dipole framework.

Saturation is usually understood as combined effects: gluon recombinations via non-linearities in the evolution equation due to x being small [47], and the importance of multiple scatterings due to the large gluon occupancy number for dense targets [35–37]. In this article, we will give a new point of view on saturation in terms of TMD physics. In par-

JHEP10(2019)208

ticular, we will distinguish 3 origins of saturation, whose effects can be studied separately. We will also discuss the linear BFKL limit as a kinematic limit rather than a dilute limit.

We will restrict ourselves to so-called dilute-dense collisions where either the projectile is a photon (with or without virtuality), or where in a hadron-hadron collision the observed particles are forward enough for the so-called hybrid factorization ansatz [48, 49] to apply. This ansatz relies on the assumption that the incoming projectile parton was produced close enough to the projectile hadron beam to be reliably described via collinear factorization. Then the observables are described as the convolution of a collinear parton distribution with a low x amplitude where the incoming parton is treated as the projectile. The hybrid ansatz was successfully applied to one-loop order [50–59] For central production, a more involved formalism similar to the one developed in [9, 10] should be used, and will be investigated in future studies.

The article is organized as follows. In section 2 we give the computation steps to rewrite low x amplitudes in a form which is compatible with an infinite twist TMD amplitude, involving all kinematic twist corrections to the 1-body and 2-body (half-)operators. In section 3 we derive the cross section in the inclusive case, involving 2-body, 3-body and 4-body TMD distributions. We then show how PDFs appear in more inclusive observables. We also discuss inclusive diffraction. In section 4 we derive the cross section in the exclusive case, which involves a GTMD. We then show how GPDs appear for less exclusive observables. In section 5 we show how the BFKL limit can be understood as a kinematic limit in the Wandzura-Wilczek approximation, and we give predictions beyond the WW approximation in terms of 2-body, 3-body and 4-body unintegrated PDFs. Finally in section 6 we discuss how saturation can be understood in terms of TMD physics and how one kind of saturation could also appear in the kinematic BFKL limit.

Notations and conventions. We will use the most generic small x limit: s is assumed to be much larger than any other scale, and our processes are assumed to have at least one partonic hard scale Q. Any number of hard or semi-hard scales can be involved.

We define lightcone directions $+$ and $-$ such that the projectile (resp. target) has a large momentum along the $+$ direction $p_0^+ \sim \sqrt{s}$ (resp. along the $-$ direction $P^- \sim \sqrt{s}$). We denote transverse components as with a $\perp$ subscript in Minkowski space and by bold characters in Euclidean space. We will thus write scalar products as

$$x \cdot y = x^+ y^- + x^- y^+ + x_\perp \cdot y_\perp = x^+ y^- + x^- y^+ - \boldsymbol{x} \cdot \boldsymbol{y}. \tag{1.3}$$

Our treatement of low x physics relies on the covariant shockwave effective approach, very similar to the Color Glass Condensate approach. These frameworks are based on the separation of gluon fields in rapidity space: the QCD Lagrangian is separated[1] into *fast* fields ($|k^+| > e^{-Y_c} p_0^+$) and *slow* fields ($|k^+| < e^{-Y_c} p_0^+$). We will use the lightcone gauge $A^+ = 0$, in which slow fields have the form

$$A^\mu_{Y_c}(x) = \delta(x^+) A^-_{Y_c}(x_\perp) \delta^{\mu -} + O\left(m_T/\sqrt{s}\right), \tag{1.4}$$

[1]For central production in hadron-hadron collisions, additional separations would be introduced.

JHEP10(2019)208

where m_T is a typical mass in the target. Note that the $\delta(x^+)$ function is a shorthand notation to account for the fact that the field is peaked around $x^+ = 0$, and should be treated as such rather than a distribution. The slow field is then treated as an external field, which allows for multiple interactions to be resummed into path-ordered Wilson lines. For a color representation R, the finite Wilson line operators are defined as

$$\left[a^+, b^+\right]^R_{\boldsymbol{x},Y_c} \equiv \mathcal{P} e^{ig\int_{a^+}^{b^+} dz^+ T_R^a A^{a-}_{Y_c}(z^+,\boldsymbol{x})}, \tag{1.5}$$

and we define the more standard infinite lines

$$U^R_{\boldsymbol{x},Y_c} = [-\infty, +\infty]^R_{\boldsymbol{x},Y_c}\,. \tag{1.6}$$

Large logarithms of s are resummed via the Y_c evolution of the Wilson line operators, given by the B-JIMWLK hierarchy of evolution equations [1–3, 39–46] , which can be written in a compact form as the action of the JIMWLK Hamiltonian H on a functional of Wilson line operators

$$\frac{d}{dY_c}\left(U^{R_1}_{\boldsymbol{x}_1,Y_c}\dots U^{R_n}_{\boldsymbol{x}_n,Y_c}\right) = -H\cdot\left(U^{R_1}_{\boldsymbol{x}_1,Y_c}\dots U^{R_n}_{\boldsymbol{x}_n,Y_c}\right). \tag{1.7}$$

Then the observables are given as the convolution of the hard part $\mathcal{H}_{Y_c}(\boldsymbol{x}_1,\dots,\boldsymbol{x}_n)$, obtained through effective Feynman rules in the external slow (classical) field with a lower rapidity cutoff Y_c for the fast (quantum) gluon fields, and the action of Wilson line operators at rapidity Y_c on target states $\left\langle P^{(\prime)}|P\right\rangle$:

$$\mathcal{A} = \int d^2\boldsymbol{x}_1\dots d^2\boldsymbol{x}_n \mathcal{H}_{Y_c}(\boldsymbol{x}_1,\dots,\boldsymbol{x}_n)\,\frac{\left\langle P^{(\prime)}\left|U^{R_1}_{\boldsymbol{x}_1,Y_c}\dots U^{R_n}_{\boldsymbol{x}_n,Y_c}\right|P\right\rangle}{\langle P|P\rangle}, \tag{1.8}$$

where for exclusive observables $\mathcal{A}$ is the amplitude and the matrix element is off-diagonal, and for inclusive observables $\mathcal{A}$ is the cross section and the matrix element is diagonal. Throughout this article, we will drop the Y_c subscripts for reader's convenience. We will normalize our target states such that

$$\left\langle P'|P\right\rangle = 2P^-(2\pi)^3\,\delta\left(P'^- - P^-\right)\delta^2\left(\boldsymbol{P'}-\boldsymbol{P}\right), \tag{1.9}$$

and use extensively relations similar to

$$\begin{aligned}\int dx_1^+ dx_2^+ d^2\boldsymbol{x}_1 d^2\boldsymbol{x}_2\,&\frac{\left\langle P\left|\left[x_2^+,x_1^+\right]_{\boldsymbol{x}_2} F^{i-}(x_1)\left[x_1^+,x_2^+\right]_{\boldsymbol{x}_1} F^{j-}(x_2)\right|P\right\rangle}{\langle P|P\rangle}\Bigg|_{x^-_{1,2}=0}\\ &= \frac{1}{2P^-}\int dr^+ d^2\boldsymbol{r}\left\langle P\left|\left[0^+,r^+\right]_{\boldsymbol{0}} F^{i-}(r)\left[r^+,0^+\right]_{\boldsymbol{r}} F^{j-}(0)\right|P\right\rangle\Big|_{r^-=0},\end{aligned} \tag{1.10}$$

as a result of normalization (1.9) and translation invariance. We will also use the fact that in lightcone gauge $A^+ = 0$ and in the eikonal approximation given in eq. (1.4), the gluon field F^{i-} simply reads

$$F^{i-}(x) = \partial^i A^-(x). \tag{1.11}$$

JHEP10(2019)208

Finally, the connection to standard parton distributions is always obtained by using small x limits of these distributions as given by relations of type:

$$\int dr^+ d^2\boldsymbol{r} e^{ixP^-r^+} \left\langle P' \left| F^{i-}(r) \mathcal{U}^{\pm}_{[r,0]} F^{j-}(0) \mathcal{U}^{\pm}_{[0,r]} \right| P \right\rangle \Big|_{r^-=0} \tag{1.12}$$
$$\to \int dr^+ d^2\boldsymbol{r} \left\langle P' \left| F^{i-}(r) \left[r^+, \pm\infty\right]_{\boldsymbol{r}} \left[\pm\infty, 0^+\right]_{\boldsymbol{0}} F^{j-}(0) \left[0^+, \pm\infty\right]_{\boldsymbol{0}} \left[\pm\infty, r^+\right]_{\boldsymbol{r}} \right| P \right\rangle \Big|_{r^-=0},$$

where $\mathcal{U}^{\pm}_{[x,y]}$ are staple gauge links:

$$\mathcal{U}^{\pm}_{[x,y]} = \left[\left(x^+, x^-, \boldsymbol{x}\right), \left(\pm\infty, x^-, \boldsymbol{x}\right)\right] \left[\left(\pm\infty, x^-, \boldsymbol{x}\right), \left(\pm\infty, x^-, \boldsymbol{y}\right)\right] \left[\left(\pm\infty, x^-, \boldsymbol{y}\right), \left(y^+, x^-, \boldsymbol{y}\right)\right], \tag{1.13}$$

whose transverse parts are subeikonal in $A^+ = 0$ axial gauge. Noting the expression for the transverse derivative of a Wilson line operator

$$\left(\partial_i U_{\boldsymbol{b}_1}\right) = ig_s \int_{-\infty}^{+\infty} db_1^+ \left[-\infty, b_1^+\right]_{\boldsymbol{b}_1} F^{i-}\left(b_1^+, 0^-, \boldsymbol{b}_1\right) \left[b_1^+, +\infty\right]_{\boldsymbol{b}_1}, \tag{1.14}$$

and that the transverse links are subeikonal, it is possible to combine Wilson lines and derivatives of Wilson lines into TMD distributions. For example, eqs. (1.12) and (1.14) allow to write the Weizsäcker-Williams TMD, defined as in eq. (1.12) with $\mathcal{U}^+$ and $\mathcal{U}^+$ staple gauge links, in terms of Wilson lines:

$$\mathcal{F}^{(3)}_{gg}(x, k_\perp) = -\frac{4}{g^2} \int \frac{d^2\mathbf{x} d^2\mathbf{y}}{(2\pi)^3} e^{-i\mathbf{k}\cdot(\mathbf{x}-\mathbf{y})} \frac{\left\langle P \left| \mathrm{Tr}\left[\left(\partial_i U_{\mathbf{x}}\right) U^\dagger_{\mathbf{y}} \left(\partial_i U_{\mathbf{y}}\right) U^\dagger_{\mathbf{x}}\right] \right| P \right\rangle}{\langle P|P\rangle} \tag{1.15}$$

or for the dipole TMD, defined as in eq. (1.12) with $\mathcal{U}^-$ and $\mathcal{U}^+$ staple gauge links:

$$\mathcal{F}^{(1)}_{qg}(x, k_\perp) = \frac{4}{g^2} \int \frac{d^2\mathbf{x} d^2\mathbf{y}}{(2\pi)^3} e^{-i\mathbf{k}\cdot(\mathbf{x}-\mathbf{y})} \frac{\left\langle P \left| \mathrm{Tr}\left[\left(\partial_i U^\dagger_{\mathbf{x}}\right) \left(\partial_i U_{\mathbf{y}}\right)\right] \right| P \right\rangle}{\langle P|P\rangle}. \tag{1.16}$$

It also allows to write TMD distributions with more complicated gauge links structures, as explained in details in the recent review [24].

2 Low x amplitudes as (G)TMD amplitudes

All the computation steps which will be performed here would apply for generic shockwave amplitudes. We will restrict ourselves to processes with 1 incoming particle of momentum p_0 in color representation R_0 and 2 outgoing particles of respective momenta p_1 and p_2 and in respective color representations R_1 and R_2, in the external field of a hadronic target. In the shockwave and CGC formulations of low x physics, the amplitude for such a process has the form [17]

$$\mathcal{A} = (2\pi)\,\delta\left(p_1^+ + p_2^+ - p_0^+\right) \int d^2\boldsymbol{b}\, d^2\boldsymbol{r}\, e^{-i(\boldsymbol{q}\cdot\boldsymbol{r}) - i(\boldsymbol{k}\cdot\boldsymbol{b})} \mathcal{H}(\boldsymbol{r}) \tag{2.1}$$
$$\times \left[\left(U^{R_1}_{\boldsymbol{b}+\bar{z}\boldsymbol{r}} T^{R_0} U^{R_2}_{\boldsymbol{b}-z\boldsymbol{r}}\right) - \left(U^{R_1}_{\boldsymbol{b}} T^{R_0} U^{R_2}_{\boldsymbol{b}}\right)\right],$$

JHEP10(2019)208

where $\mathcal{H}(\boldsymbol{r})$ is the hard part, and we defined

$$\boldsymbol{k} \equiv \boldsymbol{p}_1 + \boldsymbol{p}_2, \tag{2.2}$$

and

$$\boldsymbol{q} \equiv \frac{p_1^+ \boldsymbol{p}_1 - p_2^+ \boldsymbol{p}_2}{p_1^+ + p_2^+}, \tag{2.3}$$

and where

$$z \equiv \frac{p_1+}{p_0^+}, \quad \bar{z} \equiv \frac{p_2^+}{p_0^+} = 1 - z. \tag{2.4}$$

The study we will perform here is independent on $\mathcal{H}$ and thus valid for any process with 2 outgoing particles, with or without masses or virtualities. Note that final state partons can hadronize for example via fragmentation functions, distribution amplitudes or NRQCD, without changing the validity of present study either. Also note that the true amplitude is given by the action of the Wilson line operators on target states, which we will introduce later in section 3 in the inclusive case and in section 4 in the exclusive case. For the moment, it is enough to keep the amplitude as an operator.

The equivalence we want to prove here relies on the following rewriting of Wilson lines in terms of their derivatives:

$$U^{R_1}_{\boldsymbol{b}+\bar{z}\boldsymbol{r}} = U^{R_1}_{\boldsymbol{b}} - ir^\alpha_\perp \int \frac{d^2\boldsymbol{k}_1}{(2\pi)^2} \int d^2\boldsymbol{b}_1 \, e^{-i\boldsymbol{k}_1\cdot(\boldsymbol{b}_1-\boldsymbol{b})} \frac{e^{i\bar{z}(\boldsymbol{k}_1\cdot\boldsymbol{r})} - 1}{(\boldsymbol{k}_1\cdot\boldsymbol{r})} \left(\partial_\alpha U^{R_1}_{\boldsymbol{b}_1}\right), \tag{2.5}$$

and

$$U^{R_2}_{\boldsymbol{b}-z\boldsymbol{r}} = U^{R_2}_{\boldsymbol{b}} - ir^\alpha_\perp \int \frac{d^2\boldsymbol{k}_2}{(2\pi)^2} \int d^2\boldsymbol{b}_2 \, e^{-i\boldsymbol{k}_2\cdot(\boldsymbol{b}_2-\boldsymbol{b})} \frac{e^{-iz(\boldsymbol{k}_2\cdot\boldsymbol{r})} - 1}{(\boldsymbol{k}_2\cdot\boldsymbol{r})} \left(\partial_\alpha U^{R_2}_{\boldsymbol{b}_2}\right). \tag{2.6}$$

Indeed derivatives of Wilson line operators are the main quantities to consider when trying to match the TMD formalism, as shown in [15]. The derivative of a Wilson line in color representation R is given by

$$\left(\partial_i U^R_{\boldsymbol{b}_1}\right) = ig_s \int_{-\infty}^{+\infty} db_1^+ \left[-\infty, b_1^+\right]^R_{\boldsymbol{b}_1} T^a_R F^{i-}_a \left(b_1^+, 0^-, \boldsymbol{b}_1\right) \left[b_1^+, +\infty\right]^R_{\boldsymbol{b}_1}, \tag{2.7}$$

which allows to identify the $F^{i-}_a(b_1)$ field as the actual gluon field in a TMD operator. At moderate x this gluon would be isolated from the slow gluons in the gauge links. The amplitude (2.1) can be rewritten into 3 pieces:

$$\mathcal{A} \equiv \mathcal{A}_g + \mathcal{A}^{(1)}_k + \mathcal{A}^{(2)}_k, \tag{2.8}$$

where the 3 pieces are defined respectively as

$$\begin{aligned} \mathcal{A}_g = {} & (2\pi)\,\delta\left(p_1^+ + p_2^+ - p_0^+\right) \int d^2\boldsymbol{b}\, d^2\boldsymbol{r}\, e^{-i(\boldsymbol{q}\cdot\boldsymbol{r})-i(\boldsymbol{k}\cdot\boldsymbol{b})} \mathcal{H}(\boldsymbol{r}) \\ & \times \left(U^{R_1}_{\boldsymbol{b}+\bar{z}\boldsymbol{r}} - U^{R_1}_{\boldsymbol{b}}\right) T^{R_0} \left(U^{R_2}_{\boldsymbol{b}-z\boldsymbol{r}} - U^{R_2}_{\boldsymbol{b}}\right), \end{aligned} \tag{2.9}$$

$$\begin{aligned} \mathcal{A}^{(1)}_k = {} & (2\pi)\,\delta\left(p_1^+ + p_2^+ - p_0^+\right) \int d^2\boldsymbol{b}\, d^2\boldsymbol{r}\, e^{-i(\boldsymbol{q}\cdot\boldsymbol{r})-i(\boldsymbol{k}\cdot\boldsymbol{b})} \mathcal{H}(\boldsymbol{r}) \\ & \times \left(U^{R_1}_{\boldsymbol{b}+\bar{z}\boldsymbol{r}} - U^{R_1}_{\boldsymbol{b}}\right) T^{R_0} U^{R_2}_{\boldsymbol{b}}, \end{aligned} \tag{2.10}$$

JHEP10(2019)208

and

$$\mathcal{A}_k^{(2)} = (2\pi)\,\delta\left(p_1^+ + p_2^+ - p_0^+\right) \int d^2\boldsymbol{b}\, d^2\boldsymbol{r}\, e^{-i(\boldsymbol{q}\cdot\boldsymbol{r})-i(\boldsymbol{k}\cdot\boldsymbol{b})}\mathcal{H}\left(\boldsymbol{r}\right) \times U_{\boldsymbol{b}}^{R_1} T^{R_0}\left(U_{\boldsymbol{b}-z\boldsymbol{r}}^{R_2} - U_{\boldsymbol{b}}^{R_2}\right). \tag{2.11}$$

The first piece is easy to rewrite thanks to eqs. (2.5) and (2.6):

$$\begin{aligned}\mathcal{A}_g = (2\pi)\,\delta\left(p_1^+ + p_2^+ - p_0^+\right) &\int \frac{d^2\boldsymbol{k}_1}{(2\pi)^2}\frac{d^2\boldsymbol{k}_2}{(2\pi)^2}(2\pi)^2\,\delta^2\left(\boldsymbol{k}_1+\boldsymbol{k}_2-\boldsymbol{k}\right) \\ &\times \int d^2\boldsymbol{b}_1 d^2\boldsymbol{b}_2\, e^{-i(\boldsymbol{k}_1\cdot\boldsymbol{b}_1)-i(\boldsymbol{k}_2\cdot\boldsymbol{b}_2)}\left(\partial_i U_{\boldsymbol{b}_1}^{R_1}\right) T^{R_0}\left(\partial_j U_{\boldsymbol{b}_2}^{R_2}\right) \\ &\times \int d^2\boldsymbol{r}\, e^{-i(\boldsymbol{q}\cdot\boldsymbol{r})}\left[-\boldsymbol{r}^i\boldsymbol{r}^j\mathcal{H}\left(\boldsymbol{r}\right)\frac{\left(e^{i\bar{z}(\boldsymbol{k}_1\cdot\boldsymbol{r})}-1\right)\left(e^{-iz(\boldsymbol{k}_2\cdot\boldsymbol{r})}-1\right)}{\left(\boldsymbol{k}_1\cdot\boldsymbol{r}\right)\left(\boldsymbol{k}_2\cdot\boldsymbol{r}\right)}\right].\end{aligned} \tag{2.12}$$

This contribution is perfectly compatible with an all-kinematic-twists-resummed TMD amplitude for the first subleading-twist TMD half-operator.

The second and third pieces $\mathcal{A}_k^{(1)}$ and $\mathcal{A}_k^{(2)}$ contain both 1-gluon and 2-gluon contributions. The 1-gluon contributions were extracted and resummed in [17], then compared to predictions from the kinematic-twist-resummed TMD framework developped in [60, 61] for several concrete examples. Let us recall the method which was used, and resum the 2-gluon contributions as well. Let us write the Taylor expanded form of the Wilson line operator involved in $\mathcal{A}_k^{(1)}$:

$$\left(U_{\boldsymbol{b}+\bar{z}\boldsymbol{r}}^{R_1} - U_{\boldsymbol{b}}^{R_1}\right) T^{R_0} U_{\boldsymbol{b}}^{R_2} = \sum_{n=1}^{\infty}\frac{\bar{z}^n}{n!}\left[\left(r_\perp\cdot\partial_\perp\right)^n U_{\boldsymbol{b}}^{R_1}\right] T^{R_0} U_{\boldsymbol{b}}^{R_2} \equiv \sum_{n=1}^{\infty}\mathcal{U}_n. \tag{2.13}$$

Keeping in mind that $\mathcal{U}_n$ will be integrated as $\int d^2\boldsymbol{b}\, e^{-i(\boldsymbol{k}\cdot\boldsymbol{b})}\,\mathcal{U}_n$, we can use integrations by parts to write

$$\mathcal{U}_n = \frac{-i\bar{z}\left(k_\perp\cdot r_\perp\right)}{n}\mathcal{U}_{n-1} - \frac{\bar{z}^n}{n!}\left[\left(r_\perp\cdot\partial_\perp\right)^{n-1} U_{\boldsymbol{b}}^{R_1}\right] T^{R_0}\left(r_\perp\cdot\partial_\perp\right) U_{\boldsymbol{b}}^{R_2}. \tag{2.14}$$

Then an easy recursion shows

$$\begin{aligned}\mathcal{U}_n = &\frac{\left[-i\bar{z}\left(k_\perp\cdot r_\perp\right)\right]^{n-1}}{n!}\mathcal{U}_1 \\ &- \boldsymbol{r}^i\boldsymbol{r}^j\frac{\bar{z}^n}{n!}\sum_{m=1}^{n-1}\left[i\left(\boldsymbol{k}\cdot\boldsymbol{r}\right)\right]^{n-1-m}\left[\left(r_\perp\cdot\partial_\perp\right)^{m-1}\left(\partial^i U_{\boldsymbol{b}}^{R_1}\right)\right] T^{R_0}\left(\partial^j U_{\boldsymbol{b}}^{R_2}\right).\end{aligned} \tag{2.15}$$

Using

$$\left(r_\perp\cdot\partial_\perp\right)^{m-1}\left(\partial_i U_{\boldsymbol{b}}^{R_1}\right) = \int d^2\boldsymbol{b}_1\int\frac{d^2\boldsymbol{k}_1}{(2\pi)^2}\left(i\boldsymbol{k}_1\cdot\boldsymbol{r}\right)^{m-1} e^{i\boldsymbol{k}_1\cdot(\boldsymbol{b}-\boldsymbol{b}_1)}\left(\partial_i U_{\boldsymbol{b}_1}^{R_1}\right), \tag{2.16}$$

and

$$\left(\partial_j U_{\boldsymbol{b}}^{R_2}\right) = \int d^2\boldsymbol{b}_2\int\frac{d^2\boldsymbol{k}_2}{(2\pi)^2} e^{i\boldsymbol{k}_2\cdot(\boldsymbol{b}-\boldsymbol{b}_2)}\left(\partial_j U_{\boldsymbol{b}_2}^{R_2}\right), \tag{2.17}$$

JHEP10(2019)208

one can obtain

$$\mathcal{U}_n = \frac{\left[i\bar{z}\left(\boldsymbol{k}\cdot\boldsymbol{r}\right)\right]^{n-1}}{n!}\mathcal{U}_1 - \boldsymbol{r}^i\boldsymbol{r}^j\frac{\bar{z}^2}{n!}\int\frac{d^2\boldsymbol{k}_1}{(2\pi)^2}\frac{d^2\boldsymbol{k}_2}{(2\pi)^2}e^{i(\boldsymbol{k}_1+\boldsymbol{k}_2)\cdot\boldsymbol{b}}\int d^2\boldsymbol{b}_1 d^2\boldsymbol{b}_2\, e^{-i(\boldsymbol{k}_1\cdot\boldsymbol{b}_1)-i(\boldsymbol{k}_2\cdot\boldsymbol{b}_2)}$$
$$\times\sum_{m=1}^{n-1}\left[i\bar{z}\left(\boldsymbol{k}\cdot\boldsymbol{r}\right)\right]^{n-1-m}\left(i\bar{z}\boldsymbol{k}_1\cdot\boldsymbol{r}\right)^{m-1}\left(\partial_i U^{R_1}_{\boldsymbol{b}_1}\right)T^{R_0}\left(\partial_j U^{R_2}_{\boldsymbol{b}_2}\right). \tag{2.18}$$

A final resummation, using the relations

$$\sum_{n=1}^{\infty}\frac{X^{n-1}}{n!} = \frac{e^X-1}{X}, \tag{2.19}$$

and

$$\sum_{n=1}^{\infty}\sum_{m=1}^{n-1}\frac{X^{m-1}Y^{n-1-m}}{n!} = \frac{Y\left(e^X-1\right)-X\left(e^Y-1\right)}{XY\left(X-Y\right)}, \tag{2.20}$$

leads to

$$\left(U^{R_1}_{\boldsymbol{b}+\bar{z}\boldsymbol{r}}-U^{R_1}_{\boldsymbol{b}}\right)T^{R_0}U^{R_2}_{\boldsymbol{b}} = i\boldsymbol{r}^i\frac{e^{i\bar{z}(\boldsymbol{k}\cdot\boldsymbol{r})}-1}{(\boldsymbol{k}\cdot\boldsymbol{r})}\left(\partial^i U^{R_1}_{\boldsymbol{b}}\right)T^{R_0}U^{R_2}_{\boldsymbol{b}} \tag{2.21}$$
$$-\boldsymbol{r}^i\boldsymbol{r}^j\int\frac{d^2\boldsymbol{k}_1}{(2\pi)^2}\frac{d^2\boldsymbol{k}_2}{(2\pi)^2}e^{i(\boldsymbol{k}_1+\boldsymbol{k}_2)\cdot\boldsymbol{b}}\int d^2\boldsymbol{b}_1 d^2\boldsymbol{b}_2\, e^{-i(\boldsymbol{k}_1\cdot\boldsymbol{b}_1)-i(\boldsymbol{k}_2\cdot\boldsymbol{b}_2)}$$
$$\times\frac{(\boldsymbol{k}\cdot\boldsymbol{r})\left(e^{i\bar{z}(\boldsymbol{k}_1\cdot\boldsymbol{r})}-1\right)-(\boldsymbol{k}_1\cdot\boldsymbol{r})\left(e^{i\bar{z}(\boldsymbol{k}\cdot\boldsymbol{r})}-1\right)}{(\boldsymbol{k}_1\cdot\boldsymbol{r})(\boldsymbol{k}\cdot\boldsymbol{r})(\boldsymbol{k}-\boldsymbol{k}_1)\cdot\boldsymbol{r}}\left(\partial_i U^{R_1}_{\boldsymbol{b}_1}\right)T^{R_0}\left(\partial_j U^{R_2}_{\boldsymbol{b}_2}\right).$$

Plugging (2.21) into (2.9) finally yields

$$\mathcal{A}^{(1)}_k = (2\pi)\,\delta\left(p_1^+ + p_2^+ - p_0^+\right)\int d^2\boldsymbol{b}\, e^{-i(\boldsymbol{k}\cdot\boldsymbol{b})}\left(\partial^i U^{R_1}_{\boldsymbol{b}}\right)T^{R_0}U^{R_2}_{\boldsymbol{b}}$$
$$\times\left[i\int d^2\boldsymbol{r}\, e^{-i(\boldsymbol{q}\cdot\boldsymbol{r})}\boldsymbol{r}^i\mathcal{H}\left(\boldsymbol{r}\right)\left(\frac{e^{i\bar{z}(\boldsymbol{k}\cdot\boldsymbol{r})}-1}{(\boldsymbol{k}\cdot\boldsymbol{r})}\right)\right]$$
$$+(2\pi)\,\delta\left(p_1^+ + p_2^+ - p_0^+\right)\int\frac{d^2\boldsymbol{k}_1}{(2\pi)^2}\frac{d^2\boldsymbol{k}_2}{(2\pi)^2}(2\pi)^2\,\delta\left(\boldsymbol{k}_1+\boldsymbol{k}_2-\boldsymbol{k}\right) \tag{2.22}$$
$$\times\int d^2\boldsymbol{b}_1 d^2\boldsymbol{b}_2\, e^{-i(\boldsymbol{k}_1\cdot\boldsymbol{b}_1)-i(\boldsymbol{k}_2\cdot\boldsymbol{b}_2)}\left(\partial^i U^{R_1}_{\boldsymbol{b}_1}\right)T^{R_0}\left(\partial^j U^{R_2}_{\boldsymbol{b}_2}\right)$$
$$\times\left[\int d^2\boldsymbol{r}\, e^{-i(\boldsymbol{q}\cdot\boldsymbol{r})}\boldsymbol{r}^i\boldsymbol{r}^j\mathcal{H}\left(\boldsymbol{r}\right)\frac{(\boldsymbol{k}_1\cdot\boldsymbol{r})\left(e^{i\bar{z}(\boldsymbol{k}\cdot\boldsymbol{r})}-1\right)-(\boldsymbol{k}\cdot\boldsymbol{r})\left(e^{i\bar{z}(\boldsymbol{k}_1\cdot\boldsymbol{r})}-1\right)}{(\boldsymbol{k}_1\cdot\boldsymbol{r})(\boldsymbol{k}_2\cdot\boldsymbol{r})(\boldsymbol{k}\cdot\boldsymbol{r})}\right],$$

where a 1-gluon contribution and a 2-gluon contribution were explicitely extracted and power-resummed. Applying exactly the same method to the remaining piece, we obtain

$$\mathcal{A}^{(2)}_k = (2\pi)\,\delta\left(p_1^+ + p_2^+ - p_0^+\right)\int d^2\boldsymbol{b}\, e^{-i(\boldsymbol{k}\cdot\boldsymbol{b})}U^{R_1}_{\boldsymbol{b}}T^{R_0}\left(\partial^i U^{R_2}_{\boldsymbol{b}}\right)$$
$$\times\left[i\int d^2\boldsymbol{r}\, e^{-i(\boldsymbol{q}\cdot\boldsymbol{r})}\boldsymbol{r}^i\mathcal{H}\left(\boldsymbol{r}\right)\frac{e^{-iz(\boldsymbol{k}\cdot\boldsymbol{r})}-1}{(\boldsymbol{k}\cdot\boldsymbol{r})}\right]$$

JHEP10(2019)208

$$+ (2\pi)\,\delta\left(p_1^+ + p_2^+ - p_0^+\right) \int \frac{d^2\boldsymbol{k}_1}{(2\pi)^2}\frac{d^2\boldsymbol{k}_2}{(2\pi)^2}\,(2\pi)^2\,\delta^2\left(\boldsymbol{k}_1+\boldsymbol{k}_2-\boldsymbol{k}\right) \tag{2.23}$$
$$\times \int d^2\boldsymbol{b}_1 d^2\boldsymbol{b}_2\, e^{-i(\boldsymbol{k}_1\cdot\boldsymbol{b}_1)-i(\boldsymbol{k}_2\cdot\boldsymbol{b}_2)} \left(\partial^i U^{R_1}_{\boldsymbol{b}_1}\right) T^{R_0} \left(\partial^j U^{R_2}_{\boldsymbol{b}_2}\right)$$
$$\times \left[\int d^2\boldsymbol{r}\, e^{-i(\boldsymbol{q}\cdot\boldsymbol{r})}\mathcal{H}\left(\boldsymbol{r}\right)\boldsymbol{r}^i\boldsymbol{r}^j \frac{(\boldsymbol{k}_2\cdot\boldsymbol{r})\left(e^{-iz(\boldsymbol{k}\cdot\boldsymbol{r})}-1\right)-(\boldsymbol{k}\cdot\boldsymbol{r})\left(e^{-iz(\boldsymbol{k}_2\cdot\boldsymbol{r})}-1\right)}{(\boldsymbol{k}_1\cdot\boldsymbol{r})(\boldsymbol{k}_2\cdot\boldsymbol{r})(\boldsymbol{k}\cdot\boldsymbol{r})}\right].$$

We can finally gather the 1-gluon and 2-gluon amplitudes. The 1-gluon amplitude reads:

$$\mathcal{A}_1 = (2\pi)\,\delta\left(p_1^+ + p_2^+ - p_0^+\right)\int d^2\boldsymbol{b}\, e^{-i(\boldsymbol{k}\cdot\boldsymbol{b})}(-i)\int d^2\boldsymbol{r}\, e^{-i(\boldsymbol{q}\cdot\boldsymbol{r})} r_\perp^\alpha \mathcal{H}\left(\boldsymbol{r}\right) \tag{2.24}$$
$$\times \left[\left(\frac{e^{i\bar{z}(\boldsymbol{k}\cdot\boldsymbol{r})}-1}{(\boldsymbol{k}\cdot\boldsymbol{r})}\right)\left(\partial_\alpha U^{R_1}_{\boldsymbol{b}}\right) T^{R_0} U^{R_2}_{\boldsymbol{b}} + \left(\frac{e^{-iz(\boldsymbol{k}\cdot\boldsymbol{r})}-1}{(\boldsymbol{k}\cdot\boldsymbol{r})}\right) U^{R_1}_{\boldsymbol{b}} T^{R_0}\left(\partial_\alpha U^{R_2}_{\boldsymbol{b}}\right)\right].$$

Single-scattering contributions like those in eq. (2.24) were extracted for explicit processes in [17] and the consistency of the results was checked by comparing single-scattering cross sections derived with our method to those obtained in the so-called improved TMD formalism, which is a method to incorporate kinematic twists in TMD factorization. A perfect match was found for all processes considered.

The 2-gluon amplitude is given by:

$$\mathcal{A}_2 = (2\pi)\,\delta\left(p_1^+ + p_2^+ - p_0^+\right)\int \frac{d^2\boldsymbol{k}_1}{(2\pi)^2}\frac{d^2\boldsymbol{k}_2}{(2\pi)^2}\,(2\pi)^2\,\delta^2\left(\boldsymbol{k}_1+\boldsymbol{k}_2-\boldsymbol{k}\right)$$
$$\times \int d^2\boldsymbol{b}_1 d^2\boldsymbol{b}_2 e^{-i(\boldsymbol{k}_1\cdot\boldsymbol{b}_1)-i(\boldsymbol{k}_2\cdot\boldsymbol{b}_2)} \left(\partial^i U^{R_1}_{\boldsymbol{b}_1}\right) T^{R_0}\left(\partial^j U^{R_2}_{\boldsymbol{b}_2}\right) \tag{2.25}$$
$$\times \left[-\int d^2\boldsymbol{r} e^{-i(\boldsymbol{q}\cdot\boldsymbol{r})}\boldsymbol{r}^i\boldsymbol{r}^j\mathcal{H}\left(\boldsymbol{r}\right)\left(\frac{e^{-iz(\boldsymbol{k}\cdot\boldsymbol{r})}}{(\boldsymbol{k}\cdot\boldsymbol{r})}\frac{e^{i(\boldsymbol{k}_1\cdot\boldsymbol{r})}-1}{(\boldsymbol{k}_1\cdot\boldsymbol{r})} + \frac{e^{i\bar{z}(\boldsymbol{k}\cdot\boldsymbol{r})}}{(\boldsymbol{k}\cdot\boldsymbol{r})}\frac{e^{-i(\boldsymbol{k}_2\cdot\boldsymbol{r})}-1}{(\boldsymbol{k}_2\cdot\boldsymbol{r})}\right)\right].$$

The crucial point to note is that eqs. (2.24), (2.25) sum up exactly to the low x amplitude in (2.1). As a result, we showed that any low x amplitude of the form of eq. (2.1) can be rewritten as the sum of all kinematic twist corrections to the single-scattering (G)TMD amplitude and to the double-scattering (G)TMD amplitude (i.e. the first genuine twist correction). The notable absence of triple or higher scattering amplitudes is due to the eikonal approximation: a contribution with two derivatives hitting the same line i.e. with 2 low x TMD gluons hitting the same parton, constitutes a gauge invariance fixing contribution: it was already taken into account either as part of a gauge link or as a kinematic twist correction. We thus expect a low x amplitude with n final state particles to have at most an n-scattering operator in its amplitude in the eikonal approximation. With subeikonal corrections, one could have higher genuine twist contributions.

In principle, eqs. (2.24), (2.25) conclude the long-sought equivalence between low x and moderate x formulations of factorization: modern formulations of low x amplitudes are nothing but the sum over all twists of (G)TMD amplitudes in their small x limit.

For reader's convenience, we will use more compact notations in the following sections. We introduce

$$\mathcal{I}^i_{\mathcal{H}}\left(\boldsymbol{q},\boldsymbol{p}\right) \equiv i\int d^2\boldsymbol{r}\, e^{-i(\boldsymbol{q}\cdot\boldsymbol{r})}\boldsymbol{r}^i\mathcal{H}\left(\boldsymbol{r}\right)\left(\frac{e^{i(\boldsymbol{p}\cdot\boldsymbol{r})}-1}{(\boldsymbol{p}\cdot\boldsymbol{r})}\right), \tag{2.26}$$

JHEP10(2019)208

and

$$\mathcal{J}^{ij}_{\mathcal{H}}\left(\boldsymbol{q},\boldsymbol{k},\boldsymbol{p}\right) \equiv \int d^2\boldsymbol{r}\, e^{-i(\boldsymbol{q}\cdot\boldsymbol{r})}\boldsymbol{r}^i\boldsymbol{r}^j\mathcal{H}\left(\boldsymbol{r}\right)\frac{e^{i(\boldsymbol{k}\cdot\boldsymbol{r})}\left(e^{i(\boldsymbol{p}\cdot\boldsymbol{r})}-1\right)}{\left(\boldsymbol{p}\cdot\boldsymbol{r}\right)\left(\boldsymbol{k}\cdot\boldsymbol{r}\right)}, \tag{2.27}$$

so that

$$\begin{aligned}\mathcal{A}_1 = {}& (2\pi)\,\delta\left(p_1^+ + p_2^+ - p_0^+\right)\int d^2\boldsymbol{b}\, e^{-i(\boldsymbol{k}\cdot\boldsymbol{b})} \\ & \times\left[\bar{z}\,\mathcal{I}^i_{\mathcal{H}}\left(\boldsymbol{q},\bar{z}\boldsymbol{k}\right)\left(\partial^i U^{R_1}_{\boldsymbol{b}}\right)T^{R_0}U^{R_2}_{\boldsymbol{b}} - z\,\mathcal{I}^i_{\mathcal{H}}\left(\boldsymbol{q},-z\boldsymbol{k}\right)U^{R_1}_{\boldsymbol{b}}T^{R_0}\left(\partial^i U^{R_2}_{\boldsymbol{b}}\right)\right],\end{aligned} \tag{2.28}$$

and

$$\begin{aligned}\mathcal{A}_2 = {}& (2\pi)\,\delta\left(p_1^+ + p_2^+ - p_0^+\right)\int\frac{d^2\boldsymbol{k}_1}{(2\pi)^2}\frac{d^2\boldsymbol{k}_2}{(2\pi)^2}(2\pi)^2\,\delta^2\left(\boldsymbol{k}_1+\boldsymbol{k}_2-\boldsymbol{k}\right) \\ & \times\int d^2\boldsymbol{b}_1 d^2\boldsymbol{b}_2\, e^{-i(\boldsymbol{k}_1\cdot\boldsymbol{b}_1)-i(\boldsymbol{k}_2\cdot\boldsymbol{b}_2)}\left(\partial^i U^{R_1}_{\boldsymbol{b}_1}\right)T^{R_0}\left(\partial^j U^{R_2}_{\boldsymbol{b}_2}\right) \\ & \times\left[z\mathcal{J}^{ij}_{\mathcal{H}}\left(\boldsymbol{q},-z\boldsymbol{k},\boldsymbol{k}_1\right)+\bar{z}\mathcal{J}^{ij}_{\mathcal{H}}\left(\boldsymbol{q},\bar{z}\boldsymbol{k},-\boldsymbol{k}_2\right)\right].\end{aligned} \tag{2.29}$$

3 Inclusive cross sections

It is easy to obtain inclusive cross sections from our amplitudes (2.24) and (2.25). In order to account for the possible use of our results in the hybrid factorization ansatz, we will average over incoming projectile color states, with an averaging factor $C_0 = N_c$ for a quark, $C_0 = N_c^2 - 1$ for a gluon, and $C_0 = 1$ for a photon. We will also use the rapidities y_1 and y_2 of the outcoming particles. We can distinguish 4 contributions, depending on the number of gluons in the TMD half-operator in the amplitude and in the complex conjugate amplitude.

3.1 TMD cross sections

The 2-body contribution, given by the 4 diagrams in figure 1, reads:

$$\begin{aligned}\frac{d\sigma_{11}}{dy_1 dy_2 d^2\boldsymbol{q}d^2\boldsymbol{k}} = {}& \frac{\delta\left(p_1^+ + p_2^+ - p_0^+\right)}{8\,(2\pi)\,C_0 p_0^+}\int\frac{d^2\boldsymbol{b}'}{(2\pi)^2}\frac{d^2\boldsymbol{b}}{(2\pi)^2}e^{i\boldsymbol{k}\cdot(\boldsymbol{b}'-\boldsymbol{b})} \\ & \times\Bigg[\bar{z}^2\,\mathcal{I}^i_{\mathcal{H}}\left(\boldsymbol{q},\bar{z}\boldsymbol{k}\right)\mathcal{I}^{j*}_{\mathcal{H}}\left(\boldsymbol{q},\bar{z}\boldsymbol{k}\right)\frac{\left\langle P\left|\,\mathrm{Tr}\left[\left(\partial^i U^{R_1}_{\boldsymbol{b}}\right)T^{R_0}U^{R_2}_{\boldsymbol{b}}U^{R_2\dagger}_{\boldsymbol{b}'}T^{R_0\dagger}\left(\partial^j U^{R_1\dagger}_{\boldsymbol{b}'}\right)\right]\right|P\right\rangle}{\langle P|P\rangle} \\ & - z\bar{z}\,\mathcal{I}^i_{\mathcal{H}}\left(\boldsymbol{q},\bar{z}\boldsymbol{k}\right)\mathcal{I}^{j*}_{\mathcal{H}}\left(\boldsymbol{q},-z\boldsymbol{k}\right)\frac{\left\langle P\left|\,\mathrm{Tr}\left[\left(\partial^i U^{R_1}_{\boldsymbol{b}}\right)T^{R_0}U^{R_2}_{\boldsymbol{b}}\left(\partial^j U^{R_2\dagger}_{\boldsymbol{b}'}\right)T^{R_0\dagger}U^{R_1\dagger}_{\boldsymbol{b}'}\right]\right|P\right\rangle}{\langle P|P\rangle} \\ & - z\bar{z}\,\mathcal{I}^i_{\mathcal{H}}\left(\boldsymbol{q},-z\boldsymbol{k}\right)\mathcal{I}^{j*}_{\mathcal{H}}\left(\boldsymbol{q},\bar{z}\boldsymbol{k}\right)\frac{\left\langle P\left|\,\mathrm{Tr}\left[U^{R_1}_{\boldsymbol{b}}T^{R_0}\left(\partial^i U^{R_2}_{\boldsymbol{b}}\right)U^{R_2\dagger}_{\boldsymbol{b}'}T^{R_0\dagger}\left(\partial^j U^{R_1\dagger}_{\boldsymbol{b}'}\right)\right]\right|P\right\rangle}{\langle P|P\rangle} \\ & + z^2\,\mathcal{I}^i_{\mathcal{H}}\left(\boldsymbol{q},-z\boldsymbol{k}\right)\mathcal{I}^{j*}_{\mathcal{H}}\left(\boldsymbol{q},-z\boldsymbol{k}\right)\frac{\left\langle P\left|\,\mathrm{Tr}\left[U^{R_1}_{\boldsymbol{b}}T^{R_0}\left(\partial^i U^{R_2}_{\boldsymbol{b}}\right)\left(\partial^j U^{R_2\dagger}_{\boldsymbol{b}'}\right)T^{R_0\dagger}U^{R_1\dagger}_{\boldsymbol{b}'}\right]\right|P\right\rangle}{\langle P|P\rangle}\Bigg],\end{aligned} \tag{3.1}$$

JHEP10(2019)208

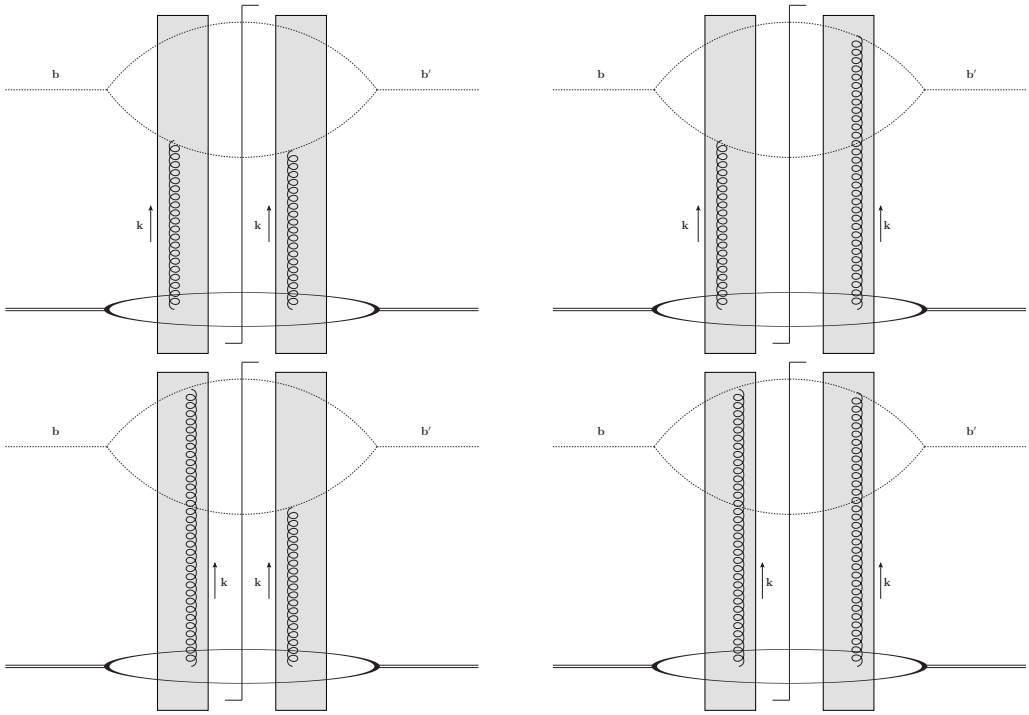

Figure 1. 2-body contributions to the inclusive cross section. The gray blobs represent interactions with low k^+ gluons via Wilson lines, and the gluon line is isolated from the gauge link contributions by differenciation of a Wilson line.

the 3-body contributions are given by the diagrams with 1 gluon in the amplitude and 2 gluons in the complex conjugate amplitude, as in figure 2, which add up to:

$$\begin{aligned}
\frac{d\sigma_{12}}{dy_1 dy_2 d^2\boldsymbol{q} d^2\boldsymbol{k}} = & \frac{\delta\left(p_1^+ + p_2^+ - p_0^+\right)}{8\left(2\pi\right) C_0 p_0^+} \int \frac{d^2\boldsymbol{k}_1'}{\left(2\pi\right)^2} \frac{d^2\boldsymbol{k}_2'}{\left(2\pi\right)^2} \left(2\pi\right)^2 \delta^2\left(\boldsymbol{k}_1' + \boldsymbol{k}_2' - \boldsymbol{k}\right) \\
& \times \int \frac{d^2\boldsymbol{b}}{\left(2\pi\right)^2} \frac{d^2\boldsymbol{b}_1' d^2\boldsymbol{b}_2'}{\left(2\pi\right)^2} e^{-i(\boldsymbol{k}\cdot\boldsymbol{b}) + i(\boldsymbol{k}_1'\cdot\boldsymbol{b}_1') + i(\boldsymbol{k}_2'\cdot\boldsymbol{b}_2')} \\
& \times \left[z \mathcal{J}_{\mathcal{H}}^{kl*}\left(\boldsymbol{q}, -z\boldsymbol{k}, \boldsymbol{k}_1'\right) + \bar{z} \mathcal{J}_{\mathcal{H}}^{kl*}\left(\boldsymbol{q}, \bar{z}\boldsymbol{k}, -\boldsymbol{k}_2'\right) \right] \\
& \times \left[\bar{z}\, \mathcal{I}_{\mathcal{H}}^{i}\left(\boldsymbol{q}, \bar{z}\boldsymbol{k}\right) \frac{\left\langle P \left| \mathrm{Tr}\left[\left(\partial^i U_{\boldsymbol{b}}^{R_1}\right) T^{R_0} U_{\boldsymbol{b}}^{R_2} \left(\partial^l U_{\boldsymbol{b}_2'}^{R_2\dagger}\right) T^{R_0\dagger} \left(\partial^k U_{\boldsymbol{b}_1'}^{R_1\dagger}\right) \right] \right| P \right\rangle}{\langle P|P\rangle} \right. \\
& \left. - z\, \mathcal{I}_{\mathcal{H}}^{i}\left(\boldsymbol{q}, -z\boldsymbol{k}\right) \frac{\left\langle P \left| \mathrm{Tr}\left[U_{\boldsymbol{b}}^{R_1} T^{R_0} \left(\partial^i U_{\boldsymbol{b}}^{R_2}\right) \left(\partial^l U_{\boldsymbol{b}_2'}^{R_2\dagger}\right) T^{R_0\dagger} \left(\partial^k U_{\boldsymbol{b}_1'}^{R_1\dagger}\right) \right] \right| P \right\rangle}{\langle P|P\rangle} \right],
\end{aligned} \tag{3.2}$$

JHEP10(2019)208

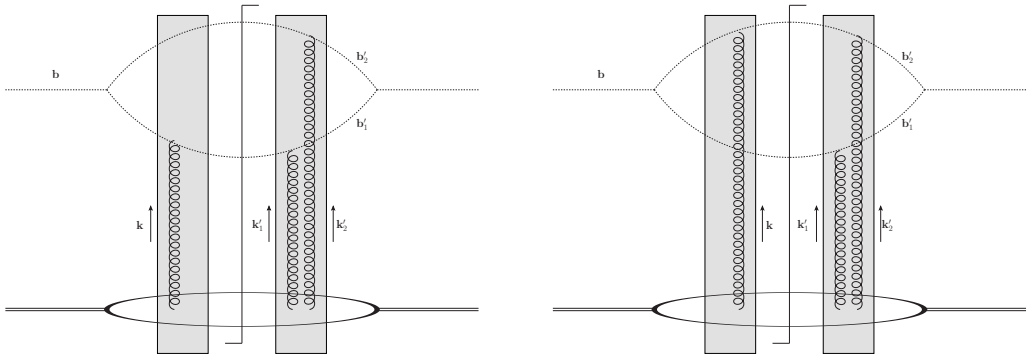

Figure 2. 3-body contributions with 2 gluons in the complex conjugate amplitude.

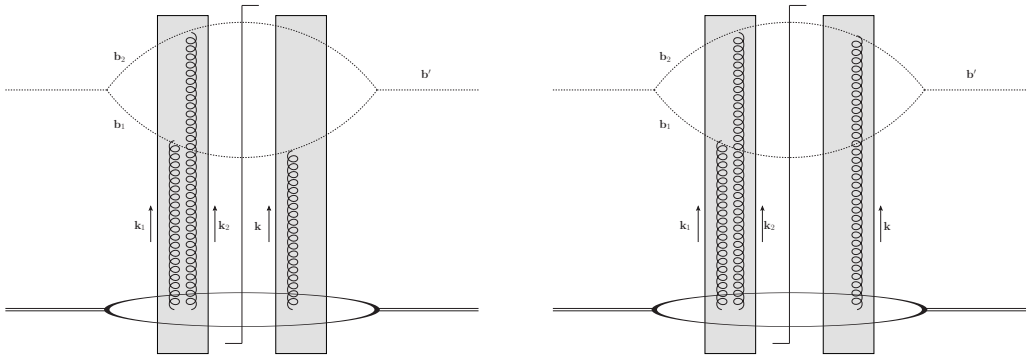

Figure 3. 3-body contributions with 2 gluons in the amplitude.

and by those with 2 gluons in the amplitude and 1 in the complex conjugate amplitude as in figure 3, which yield:

$$
\begin{aligned}
\frac{d\sigma_{21}}{dy_1 dy_2 d^2\boldsymbol{q} d^2\boldsymbol{k}} = & \frac{\delta\left(p_1^+ + p_2^+ - p_0^+\right)}{8\left(2\pi\right) C_0 p_0^+} \int \frac{d^2\boldsymbol{k}_1}{\left(2\pi\right)^2} \frac{d^2\boldsymbol{k}_2}{\left(2\pi\right)^2} \left(2\pi\right)^2 \delta^2\left(\boldsymbol{k}_1 + \boldsymbol{k}_2 - \boldsymbol{k}\right) \\
& \times \int \frac{d^2\boldsymbol{b}'}{\left(2\pi\right)^2} \frac{d^2\boldsymbol{b}_1 d^2\boldsymbol{b}_2}{\left(2\pi\right)^2} e^{i(\boldsymbol{k}\cdot\boldsymbol{b}') - i(\boldsymbol{k}_1\cdot\boldsymbol{b}_1) - i(\boldsymbol{k}_2\cdot\boldsymbol{b}_2)} \\
& \times \left[z \mathcal{J}^{ij}_{\mathcal{H}}\left(\boldsymbol{q}, -z\boldsymbol{k}, \boldsymbol{k}_1\right) + \bar{z} \mathcal{J}^{ij}_{\mathcal{H}}\left(\boldsymbol{q}, \bar{z}\boldsymbol{k}, -\boldsymbol{k}_2\right) \right] \\
& \times \left[\bar{z} \mathcal{I}^{k*}_{\mathcal{H}}\left(\boldsymbol{q}, \bar{z}\boldsymbol{k}\right) \frac{\left\langle P \left| \mathrm{Tr}\left[\left(\partial^i U^{R_1}_{\boldsymbol{b}_1}\right) T^{R_0} \left(\partial^j U^{R_2}_{\boldsymbol{b}_2}\right) U^{R_2\dagger}_{\boldsymbol{b}'} T^{R_0\dagger} \left(\partial^k U^{R_1\dagger}_{\boldsymbol{b}'}\right) \right] \right| P \right\rangle}{\langle P | P \rangle} \right. \\
& \left. - z \mathcal{I}^{k*}_{\mathcal{H}}\left(\boldsymbol{q}, -z\boldsymbol{k}\right) \frac{\left\langle P \left| \mathrm{Tr}\left[\left(\partial^i U^{R_1}_{\boldsymbol{b}_1}\right) T^{R_0} \left(\partial^j U^{R_2}_{\boldsymbol{b}_2}\right) \left(\partial^k U^{R_2\dagger}_{\boldsymbol{b}'}\right) T^{R_0\dagger} U^{R_1\dagger}_{\boldsymbol{b}'} \right] \right| P \right\rangle}{\langle P | P \rangle} \right] .
\end{aligned}
\tag{3.3}
$$

JHEP10(2019)208

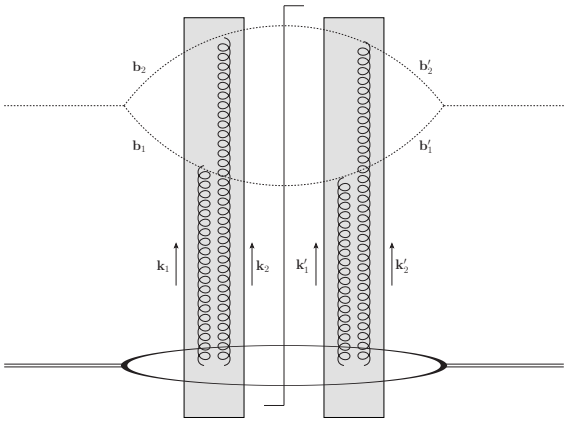

Figure 4. 4-body contribution.

Finally the 4-body contribution from the diagram in figure 4, reads

$$\begin{aligned}
\frac{d\sigma_{22}}{dy_1 dy_2 d^2\boldsymbol{q} d^2\boldsymbol{k}} &= \frac{\delta\left(p_1^+ + p_2^+ - p_0^+\right)}{8\,(2\pi)\,C_0 p_0^+} \int \frac{d^2\boldsymbol{k}_1}{(2\pi)^2}\frac{d^2\boldsymbol{k}_2}{(2\pi)^2}\,(2\pi)^2\,\delta^2\left(\boldsymbol{k}_1+\boldsymbol{k}_2-\boldsymbol{k}\right) \\
&\times \int \frac{d^2\boldsymbol{k}'_1}{(2\pi)^2}\frac{d^2\boldsymbol{k}'_2}{(2\pi)^2}\,(2\pi)^2\,\delta^2\left(\boldsymbol{k}'_1+\boldsymbol{k}'_2-\boldsymbol{k}\right) \\
&\times \int \frac{d^2\boldsymbol{b}_1 d^2\boldsymbol{b}_2}{(2\pi)^2}\frac{d^2\boldsymbol{b}'_1 d^2\boldsymbol{b}'_2}{(2\pi)^2} e^{i(\boldsymbol{k}'_1\cdot\boldsymbol{b}'_1)+i(\boldsymbol{k}'_2\cdot\boldsymbol{b}'_2)-i(\boldsymbol{k}_1\cdot\boldsymbol{b}_1)-i(\boldsymbol{k}_2\cdot\boldsymbol{b}_2)} \\
&\times \left[z\mathcal{J}^{ij}_{\mathcal{H}}\left(\boldsymbol{q},-z\boldsymbol{k},\boldsymbol{k}_1\right)+\bar{z}\mathcal{J}^{ij}_{\mathcal{H}}\left(\boldsymbol{q},\bar{z}\boldsymbol{k},-\boldsymbol{k}_2\right)\right]\left[z\mathcal{J}^{kl*}_{\mathcal{H}}\left(\boldsymbol{q},-z\boldsymbol{k},\boldsymbol{k}'_1\right)+\bar{z}\mathcal{J}^{kl*}_{\mathcal{H}}\left(\boldsymbol{q},\bar{z}\boldsymbol{k},-\boldsymbol{k}'_2\right)\right] \\
&\times \frac{\left\langle P\left|\,\mathrm{Tr}\left[\left(\partial^i U^{R_1}_{\boldsymbol{b}_1}\right)T^{R_0}\left(\partial^j U^{R_2}_{\boldsymbol{b}_2}\right)\left(\partial^l U^{R_2\dagger}_{\boldsymbol{b}'_2}\right)T^{R_0\dagger}\left(\partial^k U^{R_1\dagger}_{\boldsymbol{b}'_1}\right)\right]\right|P\right\rangle}{\langle P|P\rangle}.
\end{aligned} \tag{3.4}$$

The inclusive (or incoherent) diffractive case is very similar to the fully inclusive case. The difference lies in the TMD operators: where the fully inclusive cross section involves $\langle P|\mathrm{tr}(\mathcal{O}_{\boldsymbol{x}}\mathcal{O}^\dagger_{\boldsymbol{y}})|P\rangle$, the inclusive diffractive cross section involves $\langle P|\mathrm{tr}(\mathcal{O}^{(1)}_{\boldsymbol{x}}\mathcal{O}^{(1)\dagger}_{\boldsymbol{y}})|P\rangle$, where $\mathcal{O}^{(1)}_{\boldsymbol{x}}$ and $\mathcal{O}^{(1)\dagger}_{\boldsymbol{y}}$ are the color singlet projections of the operators. In the CGC and dipole descriptions of low x physics, this matrix element is often described as the b-dependent dipole scattering amplitude $\mathcal{N}(\boldsymbol{b},\boldsymbol{r})$. It is important to note that the $\boldsymbol{b}$ variable which appears in these matrix elements is the Fourier conjugate to the partonic transverse momentum in a TMD. As a result, it must not be interpreted as the physical impact parameter, which is the Fourier conjugate to the transverse momentum imbalance in incoming and outgoing traget states in a GTMD or GPD. Instead, the $\boldsymbol{b}$ variable involved in inclusive diffraction is actually the tranverse coordinate variable involved in the Collins-Soper equation. This remark does not invalidate the description as $\mathcal{N}\left(\boldsymbol{b},\boldsymbol{r}\right)$, but it is important to keep in mind the nature of $\boldsymbol{b}$ when interpreting this quantity for inclusive observables.

3.2 Cross sections with a PDF

A parton distribution function (PDF) is the integral of a TMD w.r.t. its partonic transverse momenta. To obtain a cross section with a PDF instead of a TMD, one

JHEP10(2019)208

should consider an inclusive process where momentum $\boldsymbol{k}$ is not measured, and expand eqs. (3.1), (3.2), (3.3), (3.4) in twists, by taking the leading power in the hard scale. Said hard scale Q can be given by a virtuality, an invariant mass... and thus the expansion is process-dependant, however we can easily see how the leading kinematic twist part of the leading genuine twist cross section (3.1) can be rewritten with a PDF: one considers $|\boldsymbol{k}| \ll Q$ in the hard factors $\mathcal{I}^i_{\mathcal{H}}$ then integrates the cross section w.r.t. $|\boldsymbol{k}|$. For example for a photon-induced process the leading twist cross section becomes:

$$\int d^2\boldsymbol{k} \left(\frac{d\sigma_{11}}{dy_1 dy_2 d^2\boldsymbol{q} d^2\boldsymbol{k}}\right)_{LT} = \frac{\alpha_s \delta\left(p_1^+ + p_2^+ - p_0^+\right)}{4C_0 p_0^+} \mathcal{I}^i_{\mathcal{H}}\left(\boldsymbol{q},\boldsymbol{0}\right) \mathcal{I}^{j*}_{\mathcal{H}}\left(\boldsymbol{q},\boldsymbol{0}\right) \times \int db^+ \left.\frac{\left\langle P\left|\,\mathrm{Tr}\left[F^{i-}\left(b\right) F^{j-}\left(0\right)\right]\right|P\right\rangle}{2P^-\left(2\pi\right)^2}\right|_{b^-=0,\boldsymbol{b}=\boldsymbol{0}}, \tag{3.5}$$

where one can easily identify a PDF in the $x \sim 0$ approximation in the second line.

4 Exclusive cross sections

4.1 GTMD cross sections

For exclusive cross sections, only the 2-body amplitudes contribute since the target matrix elements is that of a color singlet operator. The off-diagonal matrix elements of the 2-body operators can easily be identified as GTMDs. Here, we denote the momentum imbalance as $\Delta_\perp$ rather than $k_\perp$ to match more standard notations for the GTMD. The exclusive cross section reads:

$$\begin{aligned}
\frac{d\sigma_{excl}}{dy_1 dy_2 d^2\boldsymbol{q} d^2\boldsymbol{\Delta}} &= \frac{\delta\left(p_1^+ + p_2^+ - p_0^+\right)}{8\left(2\pi\right) C_0 p_0^+} \int \frac{d^2\boldsymbol{k}_1}{\left(2\pi\right)^2} \frac{d^2\boldsymbol{k}_2}{\left(2\pi\right)^2} \left(2\pi\right)^2 \delta^2\left(\boldsymbol{k}_1 + \boldsymbol{k}_2 - \boldsymbol{\Delta}\right) \\
&\times \int \frac{d^2\boldsymbol{k}'_1}{\left(2\pi\right)^2} \frac{d^2\boldsymbol{k}'_2}{\left(2\pi\right)^2} \left(2\pi\right)^2 \delta^2\left(\boldsymbol{k}'_1 + \boldsymbol{k}'_2 - \boldsymbol{\Delta}\right) \\
&\times \int \frac{d^2\boldsymbol{b}_1 d^2\boldsymbol{b}_2}{\left(2\pi\right)^2} \frac{d^2\boldsymbol{b}'_1 d^2\boldsymbol{b}'_2}{\left(2\pi\right)^2} e^{i(\boldsymbol{k}'_1\cdot\boldsymbol{b}'_1)+i(\boldsymbol{k}'_2\cdot\boldsymbol{b}'_2)-i(\boldsymbol{k}_1\cdot\boldsymbol{b}_1)-i(\boldsymbol{k}_2\cdot\boldsymbol{b}_2)} \\
&\times \left[z\mathcal{J}^{ij}_{\mathcal{H}}\left(\boldsymbol{q},-z\boldsymbol{\Delta},\boldsymbol{k}_1\right) + \bar{z}\mathcal{J}^{ij}_{\mathcal{H}}\left(\boldsymbol{q},\bar{z}\boldsymbol{\Delta},-\boldsymbol{k}_2\right)\right] \left[z\mathcal{J}^{kl*}_{\mathcal{H}}\left(\boldsymbol{q},-z\boldsymbol{\Delta},\boldsymbol{k}'_1\right) + \bar{z}\mathcal{J}^{kl*}_{\mathcal{H}}\left(\boldsymbol{q},\bar{z}\boldsymbol{\Delta},-\boldsymbol{k}'_2\right)\right] \\
&\times \mathrm{tr}_c \frac{\left\langle P-\boldsymbol{\Delta}\left|\left[\left(\partial^i U^{R_1}_{\boldsymbol{b}_1}\right) T^{R_0}\left(\partial^j U^{R_2}_{\boldsymbol{b}_2}\right)\right]^{(1)}\right|P\right\rangle}{\langle P|P\rangle} \frac{\left\langle P\left|\left[\left(\partial^l U^{R_2\dagger}_{\boldsymbol{b}'_2}\right) T^{R_0\dagger}\left(\partial^k U^{R_1\dagger}_{\boldsymbol{b}'_1}\right)\right]^{(1)}\right|P-\boldsymbol{\Delta}\right\rangle}{\langle P|P\rangle},
\end{aligned} \tag{4.1}$$

where tr_c is the trace over all remaining open color indices in the product of distributions. For example in a $g \to q\bar{q}$ cross section the last line in eq. (4.1) would read

$$\delta^{ab} \frac{\left\langle P-\boldsymbol{\Delta}\left|\frac{1}{2}\mathrm{Tr}\left[\left(\partial^i U_{\boldsymbol{b}_1}\right) T^a\left(\partial^j U^\dagger_{\boldsymbol{b}_2}\right)\right]\right|P\right\rangle}{\langle P|P\rangle} \frac{\left\langle P\left|\frac{1}{2}\mathrm{Tr}\left[\left(\partial^l U_{\boldsymbol{b}'_2}\right) T^{b\dagger}\left(\partial^k U^\dagger_{\boldsymbol{b}'_1}\right)\right]\right|P-\boldsymbol{\Delta}\right\rangle}{\langle P|P\rangle}. \tag{4.2}$$

The non-perturbative matrix elements involved in eq. (4.1) are GTMDs. We would like to emphasize the fact that eq. (4.1) is exact. Here, it shows a perfect match between exclusive low x cross sections and twist-resummed GTMD cross sections in the small x limit.

JHEP10(2019)208

4.2 Cross sections with a GPD

The GPD limit is obtained from a GTMD cross section the same way the PDF limit is obtained from a TMD cross section, noting that a GPD is the integral of a GTMD w.r.t. partonic transverse momenta. One performs a twist expansion by taking $\boldsymbol{k}_{1,2}^{(\prime)}/Q \to 0$ in the hard parts, then integrates over partonic transverse momenta. For example for photon-induced processes at leading twist:

$$\begin{aligned}\left(\frac{d\sigma_{excl}^{GPD}}{dy_1 dy_2 d^2\boldsymbol{q} d^2\boldsymbol{\Delta}}\right)_{LT} &= \frac{\alpha_s^2 \delta\left(p_1^+ + p_2^+ - p_0^+\right)}{8\left(2\pi\right) C_0 p_0^+}\left[z\mathcal{J}_{\mathcal{H}}^{ij}\left(\boldsymbol{q}, -z\boldsymbol{\Delta}, \boldsymbol{0}\right) + \bar{z}\mathcal{J}_{\mathcal{H}}^{ij}\left(\boldsymbol{q}, \bar{z}\boldsymbol{\Delta}, \boldsymbol{0}\right)\right] \\ &\times \left[z\mathcal{J}_{\mathcal{H}}^{kl*}\left(\boldsymbol{q}, -z\boldsymbol{\Delta}, \boldsymbol{0}\right) + \bar{z}\mathcal{J}_{\mathcal{H}}^{kl*}\left(\boldsymbol{q}, \bar{z}\boldsymbol{\Delta}, \boldsymbol{0}\right)\right] \\ &\times \int \frac{db^+}{2\pi P^-}\left\langle P - \boldsymbol{\Delta}\left|\mathrm{Tr}\left[F^{i-}\left(b\right)\left[b^+, 0^+\right]_{\boldsymbol{0}} F^{j-}\left(0\right)\left[0^+, b^+\right]_{\boldsymbol{0}}\right]\right| P\right\rangle\Big|_{b^-=0, \boldsymbol{b}=\boldsymbol{0}} \\ &\times \int \frac{db'^+}{2\pi P^-}\left\langle P\left|\mathrm{Tr}\left[F^{l-}\left(b'\right)\left[b'^+, 0^+\right]_{\boldsymbol{0}} F^{k-}\left(0\right)\left[0^+, b'^+\right]_{\boldsymbol{0}}\right]\right| P - \boldsymbol{\Delta}\right\rangle\Big|_{b'^-=0, \boldsymbol{b}'=\boldsymbol{0}}.\end{aligned} \tag{4.3}$$

At leading twist the gauge links do not contribute, and one can easily recognize leading twist GPDs in the last two lines.

5 The BFKL limit as a kinematic limit

The BFKL limit is usually understood as a weak field limit $gF \sim 0$, known as the dilute limit. In a previous study [17], the authors showed how this limit could also be recovered by using the Wandzura-Wilczek approximation in the CGC and identifying all gluon distributions as the unintegrated PDF, which is justified at large $|\boldsymbol{k}|$. In this section, we aim at describing the BFKL limit as a kinematic limit rather than a weak field limit. BFKL is valid when all transverse momenta are of the order of the hard scale, and we want to study BFKL beyond the WW approximation, so let us consider the limit of large partonic transverse momenta. By Fourier conjugation, this limit leads to the shrinking of transverse gauge links:

$$\left[x^+, \pm\infty\right]_{\boldsymbol{b}_i}\left[\pm\infty, y^+\right]_{\boldsymbol{b}_j} \sim \left[x^+, y^+\right]_{\boldsymbol{b}_i \sim \boldsymbol{b}_j \sim \boldsymbol{0}}. \tag{5.1}$$

This makes all gauge links unidimensional and in the same direction, which means all 2-body distributions can be rewritten as

$$\int \frac{d^2\boldsymbol{k}}{\left(2\pi\right)^2} e^{-i\left(\boldsymbol{k}\cdot\boldsymbol{x}\right)} \int dx^+ \left\langle P\left|F^{i-}\left(x\right)\left[x^+, 0^+\right]_{\boldsymbol{0}} F^{j-}\left(0\right)\left[0^+, x^+\right]_{\boldsymbol{0}}\right| P\right\rangle\Big|_{x^-=0} \tag{5.2}$$

since the modification of gauge links between x and 0 in the transverse plane is free up to small corrections. This unique distribution is the 2-body unintegrated PDF. In $A^+ = 0$ gauge, it can be rewritten as

$$\int \frac{d^2\boldsymbol{k}}{\left(2\pi\right)^2} e^{-i\left(\boldsymbol{k}\cdot\boldsymbol{x}\right)} \frac{\boldsymbol{k}^i \boldsymbol{k}^j}{\boldsymbol{k}^2} \boldsymbol{k}^2 \left\langle P\left|A^-\left(x\right)\left[x^+, 0^+\right]_{\boldsymbol{0}} A^-\left(0\right)\left[0^+, x^+\right]_{\boldsymbol{0}}\right| P\right\rangle\Big|_{x^-=0}, \tag{5.3}$$

where one can explicitely identify the so-called *nonsense polarization* vector in lightcone gauge $\frac{\boldsymbol{k}^i}{|\boldsymbol{k}|}$.

JHEP10(2019)208

The importance of gauge links at small $k_\perp$ and the shrinking of all TMD distributions into the unique unintegrated PDF was observed and confirmed numerically in [21, 23].

Similarly to eq. (5.2), all 3-body distributions become

$$\int \frac{d^2\boldsymbol{k}_1}{(2\pi)^2}\frac{d^2\boldsymbol{k}_2}{(2\pi)^2}e^{-i(\boldsymbol{k}_1\cdot\boldsymbol{x}_1)-i(\boldsymbol{k}_2\cdot\boldsymbol{x}_2)}\int dx_1^+dx_2^+ \tag{5.4}$$
$$\times\left\langle P\left|F^{i-}\left(x_1\right)\left[x_1^+,x_2^+\right]_{\mathbf{0}}g_sF^{j-}\left(x_2\right)\left[x_2^+,0^+\right]_{\mathbf{0}}F^{k-}\left(0\right)\left[0^+,x_1^+\right]_{\mathbf{0}}\right|P\right\rangle\Big|_{x_{1,2}^-=0},$$

where it is important to keep g_s in the operator rather than the hard part. Indeed genuine twist corrections do not come with a perturbative g_s suppression: the g_s factor is in the non-perturbative matrix element, which means the 3-body contributions are of the same order of perturbation theory as the 2-body contributions. We are not aware of studies from the BFKL literature where such genuine higher twist, 3- and 4- Reggeon distributions are taken into account for proton impact factors. In that sense, the BFKL limit for hadronic targets can be understood as a Wandzura-Wilczek approximation, as already observed in [17]. This approximation can be interpreted as a non-perturbative weak field approximation: it is the non-quantifiable hypothesis that $gF^{\mu\nu}\ll 1$ in the non-perturbative target. Here, we would like to emphasize that this approximation does not lead to the power expansion of gauge links which is performed to obtain the so-called dilute limit in the Color Glass Condensate framework. Instead, we observe that the gauge link structure is kinematically suppressed in the large momentum transfer regime, regardless of how $gF^{\mu\nu}$ scales like in the target. Understanding BFKL as a kinematic limit means that all genuine twist corrections should be taken into account. For example for photon-induced processes in the BFKL kinematic limit and in axial gauge, eqs. (3.1), (3.2), (3.3), (3.4) become respectively the 2-body contribution

$$\frac{d\sigma_{11}}{dy_1dy_2d^2\boldsymbol{q}d^2\boldsymbol{k}}\sim\frac{\alpha_s\delta\left(p_1^++p_2^+-p_0^+\right)}{4\left(2\pi\right)C_0p_0^+}\frac{\boldsymbol{k}^i\boldsymbol{k}^j}{\boldsymbol{k}^2}$$
$$\times\left[\bar{z}\,\mathcal{I}_{\mathcal{H}}^i\left(\boldsymbol{q},\bar{z}\boldsymbol{k}\right)+z\,\mathcal{I}_{\mathcal{H}}^i\left(\boldsymbol{q},-z\boldsymbol{k}\right)\right]\left[\bar{z}\,\mathcal{I}_{\mathcal{H}}^{j*}\left(\boldsymbol{q},\bar{z}\boldsymbol{k}\right)+z\,\mathcal{I}_{\mathcal{H}}^{j*}\left(\boldsymbol{q},-z\boldsymbol{k}\right)\right] \tag{5.5}$$
$$\times\frac{\boldsymbol{k}^2}{2P^-}\int\frac{d^2\boldsymbol{b}}{(2\pi)^2}e^{-i(\boldsymbol{k}\cdot\boldsymbol{b})}\int\frac{db^+}{2\pi}\left\langle P\left|\mathrm{Tr}\left[A^-\left(b\right)\left[b^+,0^+\right]_{\mathbf{0}}A^-\left(0\right)\left[0^+,b^+\right]_{\mathbf{0}}\right]\right|P\right\rangle\Big|_{b^-=0},$$

the 3-body contributions

$$\frac{d\sigma_{12}}{dy_1dy_2d^2\boldsymbol{q}d^2\boldsymbol{k}}=\frac{\alpha_s\delta\left(p_1^++p_2^+-p_0^+\right)}{4C_0p_0^+}\int\frac{d^2\boldsymbol{k}_1'}{(2\pi)^2}\frac{d^2\boldsymbol{k}_2'}{(2\pi)^2}\left(2\pi\right)^2\delta^2\left(\boldsymbol{k}_1'+\boldsymbol{k}_2'-\boldsymbol{k}\right) \tag{5.6}$$
$$\times\left(\frac{\boldsymbol{k}^i\boldsymbol{k}_1'^k\boldsymbol{k}_2'^l}{\boldsymbol{k}^2}\right)\left[\bar{z}\,\mathcal{I}_{\mathcal{H}}^i\left(\boldsymbol{q},\bar{z}\boldsymbol{k}\right)+z\,\mathcal{I}_{\mathcal{H}}^i\left(\boldsymbol{q},-z\boldsymbol{k}\right)\right]\left[\bar{z}\mathcal{J}_{\mathcal{H}}^{kl*}\left(\boldsymbol{q},\bar{z}\boldsymbol{k},-\boldsymbol{k}_2'\right)+z\mathcal{J}_{\mathcal{H}}^{kl*}\left(\boldsymbol{q},-z\boldsymbol{k},\boldsymbol{k}_1'\right)\right]$$
$$\times\frac{\boldsymbol{k}^2}{2P^-}\int\frac{d^2\boldsymbol{b}}{(2\pi)^2}\frac{d^2\boldsymbol{b}'}{(2\pi)^2}e^{-i(\boldsymbol{k}\cdot\boldsymbol{b})+i(\boldsymbol{k}_2'\cdot\boldsymbol{b}')}\int db^+db'^+$$
$$\times\left\langle P\left|\mathrm{Tr}\left[A^-\left(b\right)\left[b^+,b'^+\right]_{\mathbf{0}}g_sA^-\left(b'\right)\left[b'^+,0^+\right]_{\mathbf{0}}A^-\left(0\right)\left[0^+,b^+\right]_{\mathbf{0}}\right]\right|P\right\rangle\Big|_{b^{(\prime)-}=0},$$

JHEP10(2019)208

and

$$\frac{d\sigma_{21}}{dy_1 dy_2 d^2\boldsymbol{q} d^2\boldsymbol{k}} = \frac{\alpha_s \delta\left(p_1^+ + p_2^+ - p_0^+\right)}{2C_0 p_0^+} \int \frac{d^2\boldsymbol{k}_1}{(2\pi)^2} \frac{d^2\boldsymbol{k}_2}{(2\pi)^2} (2\pi)^2 \delta^2\left(\boldsymbol{k}_1 + \boldsymbol{k}_2 - \boldsymbol{k}\right) \tag{5.7}$$
$$\times \left(\frac{\boldsymbol{k}_1^i \boldsymbol{k}_2^j \boldsymbol{k}^k}{\boldsymbol{k}^2}\right) \left[\bar{z}\mathcal{J}_{\mathcal{H}}^{ij}\left(\boldsymbol{q}, \bar{z}\boldsymbol{k}, -\boldsymbol{k}_2\right) + z\mathcal{J}_{\mathcal{H}}^{ij}\left(\boldsymbol{q}, -z\boldsymbol{k}, \boldsymbol{k}_1\right)\right] \left[\bar{z}\,\mathcal{I}_{\mathcal{H}}^{k*}\left(\boldsymbol{q}, \bar{z}\boldsymbol{k}\right) + z\,\mathcal{I}_{\mathcal{H}}^{k*}\left(\boldsymbol{q}, -z\boldsymbol{k}\right)\right]$$
$$\times \frac{\boldsymbol{k}^2}{2P^-} \int \frac{d^2\boldsymbol{b}}{(2\pi)^2} \frac{d^2\boldsymbol{b}'}{(2\pi)^2} e^{-i(\boldsymbol{k}_1\cdot\boldsymbol{b}) - i(\boldsymbol{k}_2\cdot\boldsymbol{b}')} \int db^+ db'^+$$
$$\times \left\langle P \left| \mathrm{Tr}\left[A^-\left(b\right)\left[b^+, b'^+\right]_{\mathbf{0}} g_s A^-\left(b'\right)\left[b'^+, 0^+\right]_{\mathbf{0}} A^-\left(0\right)\left[0^+, b^+\right]_{\mathbf{0}}\right] \right| P \right\rangle \right|_{b^{(\prime)-}=0},$$

and finally the 4-body contribution

$$\frac{d\sigma_{22}}{dy_1 dy_2 d^2\boldsymbol{q} d^2\boldsymbol{k}} = \frac{\alpha_s \delta\left(p_1^+ + p_2^+ - p_0^+\right)}{2C_0 p_0^+} \int \frac{d^2\boldsymbol{k}_1}{(2\pi)^2} \frac{d^2\boldsymbol{k}_2}{(2\pi)^2} (2\pi)^2 \delta\left(\boldsymbol{k}_1 + \boldsymbol{k}_2 - \boldsymbol{k}\right)$$
$$\times \int \frac{d^2\boldsymbol{k}_1'}{(2\pi)^2} \frac{d^2\boldsymbol{k}_2'}{(2\pi)^2} (2\pi)^2 \delta\left(\boldsymbol{k}_1' + \boldsymbol{k}_2' - \boldsymbol{k}\right) \tag{5.8}$$
$$\times \frac{\boldsymbol{k}_1^i \boldsymbol{k}_2^j}{\boldsymbol{k}^2} \left[z\mathcal{J}_{\mathcal{H}}^{ij}\left(\boldsymbol{q}, -z\boldsymbol{k}, \boldsymbol{k}_1\right) + \bar{z}\mathcal{J}_{\mathcal{H}}^{ij}\left(\boldsymbol{q}, \bar{z}\boldsymbol{k}, -\boldsymbol{k}_2\right)\right]$$
$$\times \frac{\boldsymbol{k}_1'^k \boldsymbol{k}_2'^l}{\boldsymbol{k}^2} \left[z\mathcal{J}_{\mathcal{H}}^{kl*}\left(\boldsymbol{q}, -z\boldsymbol{k}, \boldsymbol{k}_1'\right) + \bar{z}\mathcal{J}_{\mathcal{H}}^{kl*}\left(\boldsymbol{q}, \bar{z}\boldsymbol{k}, -\boldsymbol{k}_2'\right)\right]$$
$$\times \int \frac{d^2\boldsymbol{b}_1 d^2\boldsymbol{b}_2}{(2\pi)^2} \frac{d^2\boldsymbol{b}'}{(2\pi)^2} e^{i(\boldsymbol{k}_2'\cdot\boldsymbol{b}') - i(\boldsymbol{k}_1\cdot\boldsymbol{b}_1) - i(\boldsymbol{k}_2\cdot\boldsymbol{b}_2)} \int db_1^+ db_2^+ db'^+$$
$$\times \frac{\boldsymbol{k}^4}{2P^-} \Big\langle P \Big| \mathrm{Tr}\Big(A^-\left(b_1\right)\left[b_1^+, b_2^+\right]_{\mathbf{0}} g_s A^-\left(b_2\right)\left[b_2^+, b'^+\right]_{\mathbf{0}}$$
$$\times g_s A^-\left(b'\right)\left[b'^+, 0^+\right]_{\mathbf{0}} A^-\left(0\right)\left[0^+, b_1^+\right]_{\mathbf{0}}\Big) \Big| P \Big\rangle \Big|_{b_{1,2}^- = b'^- = 0}.$$

We emphasize that all 4 contributions are of the same order in perturbation theory, and neglecting the contributions from genuine higher twist unintegrated PDFs is justified as a Wandzura-Wilczek approximation rather than a perturbative suppression. The validity of this approximation should be evaluated for each process. For example if one considers the production of a dijet in Deep Inelastic Scattering at large momentum transfer, deviations from Leading Logarithmic BFKL predictions could be due to the non-validity of the Wandzura Wilczek approximation, at the same perturbative order. On the other hand since the large momentum transfer is what is usually understood as the dilute regime in the Color Glass Condensate, the 3- and 4- body contributions would also be missing from the perturbative expansion of the Wilson lines unless the WW approximation is valid. Since there is no model independent way to estimate the validity this approximation, only comparisons of present results to data will confirm whether genuine higher twists could be neglected at large momentum transfer.

6 The origins of saturation

In our formulation of low x physics, saturation can be understood as 3 distinct effects.

JHEP10(2019)208

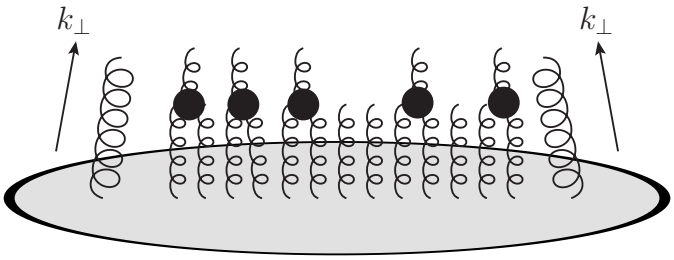

Figure 5. Saturation effects from the evolution: the non-linearities in the evolution equation account for recombination effects in the target.

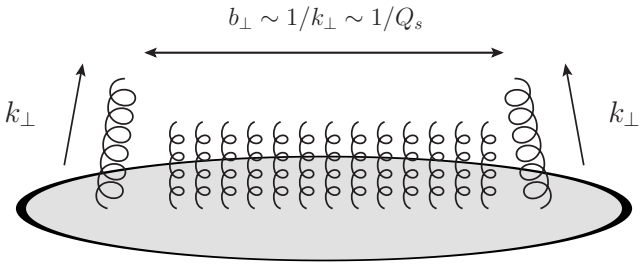

Figure 6. Kinematic saturation: the separation between the TMD gluons is filled by multiple soft scatterings.

First of all, a well known form of saturation is evolutional, and arises from the non-linearity of the B-JIMWLK hierarchy of evolution equations and its truncated and approximated daughter equations. See figure 5. This non-linearity is expected to slow down the growth in s of low x cross sections [47], thus contributing to restoring the Froissart bound.

The other effects are due to multiple scattering via interactions with slow gluons, but we will distinguish two types of such effects. We will refer to the first type, described in figure 6, as the *kinematic saturation*. It is linked to the gauge link structures of the gluon distributions. Indeed, the gauge links account for multiple scatterings from slow gluons, and the importance of such gauge links are, in that sense, a probe for multiple scattering effects. These effects were recently investigated in [21, 23]. They are expected to appear at small $|\boldsymbol{k}|$, since all TMD distributions reduce to the unintegrated PDF in the large $|\boldsymbol{k}|$ limit regardless of their gauge link structure, as discussed earlier. By studying the behavior of different distributions all along the $|\boldsymbol{k}|$ range, it was shown that indeed distributions with distinct gauge link structures have to be distinguished at low $|\boldsymbol{k}|$ while at large $|\boldsymbol{k}|$ all distributions are the same. This kind of multiple scattering is thus due to the presence of a large transverse coordinate region, conjugate to $|\boldsymbol{k}|$, to fill with the soft gluons in that kinematic regime.

Finally the last type of saturation, described in figure 7, to which we will refer as *genuine saturation*, is due to genuine twist corrections. In addition to the gluons forming the gauge links, the extra gluons from higher twist operators can contribute to multiple scattering effects. Given that the genuine twist corrections in an operator are obtained in physical gauges by the insertion of a gluon field along with the coupling constant g_s and the appropriate gauge links, the genuine twist corrections are not perturbatively suppressed as

JHEP10(2019)208

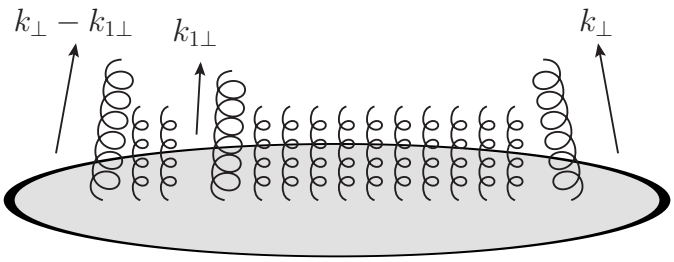

Figure 7. Genuine saturation: for dense targets where gluon occupancy is large, the probability to extract more gluons is enhanced, hence an expected enhancement of genuine twist corrections.

assumed implicitely in most studies involving unintegrated PDFs:[2] the g_s factor is part of the non-perturbative matrix elements and neglecting them is tantamount to using the Wandzura-Wilczek approximation. This kind of saturation effects would appear even in the high $|\boldsymbol{k}|$ BFKL regime if one does not restrict oneself to this unquantified approximation, whose validity should be tested in a process-dependent way. In the CGC picture, the large gluon occupancy number in a dense target leads to the scaling $g_s F \sim 1$, which leads to an expected enhancement of genuine twist corrections. In that sense, genuine saturation can be understood as the invalidation of the Wandzura-Wilczek approximation.

7 Discussion

We have found that any low x cross section for a process of type $p_0 H \to p_1 p_2 X$, where H is a hadron and X remnants are not measured, can be rewritten into an infinite twist TMD cross section. Similarly, any low x exclusive cross section for a process of type $p_0 H \to p_1 p_2 H'$, where H (resp. H') is an incoming (resp. outgoing) hadron, was rewritten into an infinite twist GTMD cross section. All the steps which were involved in this study could be applied for processes with more than 2 particles in the final state, or more than 1 in the initial state. We thus bridged one of the main gaps between low x and moderate x formulations of perturbative QCD: the apparent difference between the involved non-perturbative matrix elements.

We have also given a new interpretation of saturation in the low x regime and distinguished 3 types of saturation: evolutional, kinematic and genuine.

Each type of saturation can in principle be studied separately from the others, and there are easy ways to distinguish them. For example studying high $|\boldsymbol{k}|$ processes on dense targets and on dilute targets would probe genuine saturation alone. Small $|\boldsymbol{k}|$ observables would be probes of both genuine and kinematic saturation on dense targets, and of kinematic saturation alone on dilute targets.

Angular correlations can be studied similarly to [20], in the whole kinematic range in $|\boldsymbol{k}|$ using our results and a tensorial decomposition of the involved TMD distributions.

[2] Obviously this remark only concerns non-perturbative targets. BFKL resummation is valid in full generality for soft gluon exchanges between perturbative objects, for example Mueller Navelet jets [62].

JHEP10(2019)208

It would be very insightful in future studies to focus on subeikonal corrections to low x physics and try to match a TMD framework, similarly to what was performed in this article.

Subeikonal corrections should be particularly interesting to study in terms of (G)TMD distributions. There is no reason to believe that beyond the eikonal limit, the distributions can be exponentiated into simple Wilson lines. Rather, they will be given as what was named *decorated Wilson lines* in [4–6, 63], see also [11]. The most interesting correction to the small x limit of TMD distributions will be the phases xP^-r^+ from eq. (1.12). Beyond the leading twist, contributions with more than two physical TMD gluon will have more than one of such phases, rendering them explicitely distinct from the leading genuine twist distributions, even when written as derivatives of Wilson lines as in eq. (2.25). Subeikonal phases in eqs. (2.24), (2.25) are thus the origin of the breaking of exponentiation. On the other hand, the present computation proved that in the eikonal approximation, there is at most two physical TMD gluons for processes with two fast partons. This means that there is only a finite number of genuine twist corrections. This observation might be broken beyond the eikonal approximation, which would make it extremely difficult to work directly at infinite twist as is done in the eikonal limit.

Finally, the most powerful feature of our formulation in terms of standard parton distributions is the possibility to resum easily logarithms of Q and $|\boldsymbol{k}|$ using the known evolution equations for TMD distributions and Sudakov resummations. This could help solve the observed negativity issues for low x cross sections (see for example [52, 53, 55, 56]). Indeed the resummation of collinear logarithms via a similarly collinearly-improved low x evolution equation [64–67] is one of the most efficient tools to deal with the issue. A complementary approach to the improved-JIMWLK evolution would be to first apply the Y_c evolution using the regular JIMWLK equation, then rewrite the evolved observables in terms of TMD distributions as was done in this article, and finally resum logarithms of the hard scale and Sudakov logarithms using standard TMD methods. For the leading twist TMD operators, one could also in principle use the evolution equations derived in [7, 8].

Acknowledgments

RB thanks L. Szymanowski, P. Taels and R. Venugopalan for stimulating discussions. TA gratefully acknowledges the support from Bourses du Gouvernement Français (BGF)-Séjour de recherche, and expresses his gratitude to CPHT, Ecole Polytechnique. The work of TA is supported by Grant No. 2017/26/M/ST2/01074 of the National Science Centre, Poland. The work of RB is supported by the U.S. Department of Energy, Office of Nuclear Physics, under Contracts No. DE-SC0012704 and by an LDRD grant from Brookhaven Science Associates.

JHEP10(2019)208

References

[1] I. Balitsky, *Operator expansion for high-energy scattering*, *Nucl. Phys.* **B 463** (1996) 99 [hep-ph/9509348] [INSPIRE].

[2] I. Balitsky, *Factorization for high-energy scattering*, *Phys. Rev. Lett.* **81** (1998) 2024 [hep-ph/9807434] [INSPIRE].

[3] I. Balitsky, *Factorization and high-energy effective action*, *Phys. Rev.* **D 60** (1999) 014020 [hep-ph/9812311] [INSPIRE].

[4] T. Altinoluk, N. Armesto, G. Beuf, M. Martínez and C.A. Salgado, *Next-to-eikonal corrections in the CGC: gluon production and spin asymmetries in pA collisions*, *JHEP* **07** (2014) 068 [arXiv:1404.2219] [INSPIRE].

[5] T. Altinoluk, N. Armesto, G. Beuf and A. Moscoso, *Next-to-next-to-eikonal corrections in the CGC*, *JHEP* **01** (2016) 114 [arXiv:1505.01400] [INSPIRE].

[6] T. Altinoluk and A. Dumitru, *Particle production in high-energy collisions beyond the shockwave limit*, *Phys. Rev.* **D 94** (2016) 074032 [arXiv:1512.00279] [INSPIRE].

[7] I. Balitsky and A. Tarasov, *Rapidity evolution of gluon TMD from low to moderate x*, *JHEP* **10** (2015) 017 [arXiv:1505.02151] [INSPIRE].

[8] I. Balitsky and A. Tarasov, *Gluon TMD in particle production from low to moderate x*, *JHEP* **06** (2016) 164 [arXiv:1603.06548] [INSPIRE].

[9] I. Balitsky and A. Tarasov, *Higher-twist corrections to gluon TMD factorization*, *JHEP* **07** (2017) 095 [arXiv:1706.01415] [INSPIRE].

[10] I. Balitsky and A. Tarasov, *Power corrections to TMD factorization for Z-boson production*, *JHEP* **05** (2018) 150 [arXiv:1712.09389] [INSPIRE].

[11] G.A. Chirilli, *Sub-eikonal corrections to scattering amplitudes at high energy*, *JHEP* **01** (2019) 118 [arXiv:1807.11435] [INSPIRE].

[12] Y.V. Kovchegov, D. Pitonyak and M.D. Sievert, *Helicity evolution at small-x*, *JHEP* **01** (2016) 072 [*Erratum ibid.* **10** (2016) 148] [arXiv:1511.06737] [INSPIRE].

[13] Y.V. Kovchegov, D. Pitonyak and M.D. Sievert, *Helicity evolution at small x: flavor singlet and non-singlet observables*, *Phys. Rev.* **D 95** (2017) 014033 [arXiv:1610.06197] [INSPIRE].

[14] F. Dominguez, B.-W. Xiao and F. Yuan, *k_t-factorization for hard processes in nuclei*, *Phys. Rev. Lett.* **106** (2011) 022301 [arXiv:1009.2141] [INSPIRE].

[15] F. Dominguez, C. Marquet, B.-W. Xiao and F. Yuan, *Universality of unintegrated gluon distributions at small x*, *Phys. Rev.* **D 83** (2011) 105005 [arXiv:1101.0715] [INSPIRE].

[16] T. Altinoluk, R. Boussarie, C. Marquet and P. Taels, *TMD factorization for dijets + photon production from the dilute-dense CGC framework*, *JHEP* **07** (2019) 079 [arXiv:1810.11273] [INSPIRE].

[17] T. Altinoluk, R. Boussarie and P. Kotko, *Interplay of the CGC and TMD frameworks to all orders in kinematic twist*, *JHEP* **05** (2019) 156 [arXiv:1901.01175] [INSPIRE].

[18] A. Metz and J. Zhou, *Distribution of linearly polarized gluons inside a large nucleus*, *Phys. Rev.* **D 84** (2011) 051503 [arXiv:1105.1991] [INSPIRE].

[19] E. Akcakaya, A. Schäfer and J. Zhou, *Azimuthal asymmetries for quark pair production in pA collisions*, *Phys. Rev.* **D 87** (2013) 054010 [arXiv:1208.4965] [INSPIRE].

JHEP10(2019)208

[20] A. Dumitru and V. Skokov, *cos(4φ) azimuthal anisotropy in small-x DIS dijet production beyond the leading power TMD limit*, *Phys. Rev.* **D 94** (2016) 014030 [arXiv:1605.02739] [INSPIRE].

[21] C. Marquet, E. Petreska and C. Roiesnel, *Transverse-momentum-dependent gluon distributions from JIMWLK evolution*, *JHEP* **10** (2016) 065 [arXiv:1608.02577] [INSPIRE].

[22] D. Boer, P.J. Mulders, J. Zhou and Y.-J. Zhou, *Suppression of maximal linear gluon polarization in angular asymmetries*, *JHEP* **10** (2017) 196 [arXiv:1702.08195] [INSPIRE].

[23] C. Marquet, C. Roiesnel and P. Taels, *Linearly polarized small-x gluons in forward heavy-quark pair production*, *Phys. Rev.* **D 97** (2018) 014004 [arXiv:1710.05698] [INSPIRE].

[24] E. Petreska, *TMD gluon distributions at small x in the CGC theory*, *Int. J. Mod. Phys.* **E 27** (2018) 1830003 [arXiv:1804.04981] [INSPIRE].

[25] Y. Hatta, B.-W. Xiao and F. Yuan, *Probing the small-x gluon tomography in correlated hard diffractive dijet production in deep inelastic scattering*, *Phys. Rev. Lett.* **116** (2016) 202301 [arXiv:1601.01585] [INSPIRE].

[26] R. Boussarie, Y. Hatta, B.-W. Xiao and F. Yuan, *Probing the Weizsäcker-Williams gluon Wigner distribution in pp collisions*, *Phys. Rev.* **D 98** (2018) 074015 [arXiv:1807.08697] [INSPIRE].

[27] Y. Hatta, B.-W. Xiao and F. Yuan, *Gluon tomography from deeply virtual Compton scattering at small-x*, *Phys. Rev.* **D 95** (2017) 114026 [arXiv:1703.02085] [INSPIRE].

[28] A.V. Belitsky, X.-D. Ji and F. Yuan, *Quark imaging in the proton via quantum phase space distributions*, *Phys. Rev.* **D 69** (2004) 074014 [hep-ph/0307383] [INSPIRE].

[29] C. Lorce and B. Pasquini, *Quark Wigner distributions and orbital angular momentum*, *Phys. Rev.* **D 84** (2011) 014015 [arXiv:1106.0139] [INSPIRE].

[30] E.A. Kuraev, L.N. Lipatov and V.S. Fadin, *The Pomeranchuk singularity in non-Abelian gauge theories*, *Sov. Phys. JETP* **45** (1977) 199 [*Zh. Eksp. Teor. Fiz.* **72** (1977) 377] [INSPIRE].

[31] I.I. Balitsky and L.N. Lipatov, *The Pomeranchuk singularity in quantum chromodynamics*, *Sov. J. Nucl. Phys.* **28** (1978) 822 [*Yad. Fiz.* **28** (1978) 1597] [INSPIRE].

[32] A.H. Mueller, *Small x behavior and parton saturation: a QCD model*, *Nucl. Phys.* **B 335** (1990) 115 [INSPIRE].

[33] A.H. Mueller, *Soft gluons in the infinite momentum wave function and the BFKL Pomeron*, *Nucl. Phys.* **B 415** (1994) 373 [INSPIRE].

[34] A.H. Mueller, *Unitarity and the BFKL Pomeron*, *Nucl. Phys.* **B 437** (1995) 107 [hep-ph/9408245] [INSPIRE].

[35] L.D. McLerran and R. Venugopalan, *Computing quark and gluon distribution functions for very large nuclei*, *Phys. Rev.* **D 49** (1994) 2233 [hep-ph/9309289] [INSPIRE].

[36] L.D. McLerran and R. Venugopalan, *Gluon distribution functions for very large nuclei at small transverse momentum*, *Phys. Rev.* **D 49** (1994) 3352 [hep-ph/9311205] [INSPIRE].

[37] L.D. McLerran and R. Venugopalan, *Green's functions in the color field of a large nucleus*, *Phys. Rev.* **D 50** (1994) 2225 [hep-ph/9402335] [INSPIRE].

[38] F. Gelis, E. Iancu, J. Jalilian-Marian and R. Venugopalan, *The color glass condensate*, *Ann. Rev. Nucl. Part. Sci.* **60** (2010) 463 [arXiv:1002.0333] [INSPIRE].

JHEP10(2019)208

[39] J. Jalilian-Marian, A. Kovner, A. Leonidov and H. Weigert, *The BFKL equation from the Wilson renormalization group*, *Nucl. Phys.* **B 504** (1997) 415 [hep-ph/9701284] [INSPIRE].

[40] J. Jalilian-Marian, A. Kovner, A. Leonidov and H. Weigert, *The Wilson renormalization group for low x physics: towards the high density regime*, *Phys. Rev.* **D 59** (1998) 014014 [hep-ph/9706377] [INSPIRE].

[41] J. Jalilian-Marian, A. Kovner and H. Weigert, *The Wilson renormalization group for low x physics: gluon evolution at finite parton density*, *Phys. Rev.* **D 59** (1998) 014015 [hep-ph/9709432] [INSPIRE].

[42] A. Kovner and J.G. Milhano, *Vector potential versus color charge density in low x evolution*, *Phys. Rev.* **D 61** (2000) 014012 [hep-ph/9904420] [INSPIRE].

[43] A. Kovner, J.G. Milhano and H. Weigert, *Relating different approaches to nonlinear QCD evolution at finite gluon density*, *Phys. Rev.* **D 62** (2000) 114005 [hep-ph/0004014] [INSPIRE].

[44] H. Weigert, *Unitarity at small Bjorken x*, *Nucl. Phys.* **A 703** (2002) 823 [hep-ph/0004044] [INSPIRE].

[45] E. Iancu, A. Leonidov and L.D. McLerran, *Nonlinear gluon evolution in the color glass condensate.* 1, *Nucl. Phys.* **A 692** (2001) 583 [hep-ph/0011241] [INSPIRE].

[46] E. Ferreiro, E. Iancu, A. Leonidov and L. McLerran, *Nonlinear gluon evolution in the color glass condensate.* 2, *Nucl. Phys.* **A 703** (2002) 489 [hep-ph/0109115] [INSPIRE].

[47] L.V. Gribov, E.M. Levin and M.G. Ryskin, *Semihard processes in QCD*, *Phys. Rept.* **100** (1983) 1 [INSPIRE].

[48] A. Dumitru, A. Hayashigaki and J. Jalilian-Marian, *The color glass condensate and hadron production in the forward region*, *Nucl. Phys.* **A 765** (2006) 464 [hep-ph/0506308] [INSPIRE].

[49] T. Altinoluk and A. Kovner, *Particle production at high energy and large transverse momentum — 'the hybrid formalism' revisited*, *Phys. Rev.* **D 83** (2011) 105004 [arXiv:1102.5327] [INSPIRE].

[50] G.A. Chirilli, B.-W. Xiao and F. Yuan, *One-loop factorization for inclusive hadron production in pA collisions in the saturation formalism*, *Phys. Rev. Lett.* **108** (2012) 122301 [arXiv:1112.1061] [INSPIRE].

[51] G.A. Chirilli, B.-W. Xiao and F. Yuan, *Inclusive hadron productions in pA collisions*, *Phys. Rev.* **D 86** (2012) 054005 [arXiv:1203.6139] [INSPIRE].

[52] A.M. Stasto, B.-W. Xiao and D. Zaslavsky, *Towards the test of saturation physics beyond leading logarithm*, *Phys. Rev. Lett.* **112** (2014) 012302 [arXiv:1307.4057] [INSPIRE].

[53] A.M. Staśto, B.-W. Xiao, F. Yuan and D. Zaslavsky, *Matching collinear and small x factorization calculations for inclusive hadron production in pA collisions*, *Phys. Rev.* **D 90** (2014) 014047 [arXiv:1405.6311] [INSPIRE].

[54] T. Altinoluk, N. Armesto, G. Beuf, A. Kovner and M. Lublinsky, *Single-inclusive particle production in proton-nucleus collisions at next-to-leading order in the hybrid formalism*, *Phys. Rev.* **D 91** (2015) 094016 [arXiv:1411.2869] [INSPIRE].

[55] K. Watanabe, B.-W. Xiao, F. Yuan and D. Zaslavsky, *Implementing the exact kinematical constraint in the saturation formalism*, *Phys. Rev.* **D 92** (2015) 034026 [arXiv:1505.05183] [INSPIRE].

JHEP10(2019)208

[56] B. Ducloué, T. Lappi and Y. Zhu, *Single inclusive forward hadron production at next-to-leading order*, *Phys. Rev.* **D 93** (2016) 114016 [arXiv:1604.00225] [INSPIRE].

[57] E. Iancu, A.H. Mueller and D.N. Triantafyllopoulos, *CGC factorization for forward particle production in proton-nucleus collisions at next-to-leading order*, *JHEP* **12** (2016) 041 [arXiv:1608.05293] [INSPIRE].

[58] B. Ducloué et al., *Use of a running coupling in the NLO calculation of forward hadron production*, *Phys. Rev.* **D 97** (2018) 054020 [arXiv:1712.07480] [INSPIRE].

[59] B. Ducloué, T. Lappi and Y. Zhu, *Implementation of NLO high energy factorization in single inclusive forward hadron production*, *Phys. Rev.* **D 95** (2017) 114007 [arXiv:1703.04962] [INSPIRE].

[60] P. Kotko, K. Kutak, C. Marquet, E. Petreska, S. Sapeta and A. van Hameren, *Improved TMD factorization for forward dijet production in dilute-dense hadronic collisions*, *JHEP* **09** (2015) 106 [arXiv:1503.03421] [INSPIRE].

[61] A. van Hameren, P. Kotko, K. Kutak, C. Marquet, E. Petreska and S. Sapeta, *Forward di-jet production in p+Pb collisions in the small-x improved TMD factorization framework*, *JHEP* **12** (2016) 034 [*Erratum ibid.* **02** (2019) 158] [arXiv:1607.03121] [INSPIRE].

[62] A.H. Mueller and H. Navelet, *An inclusive minijet cross-section and the bare Pomeron in QCD*, *Nucl. Phys.* **B 282** (1987) 727 [INSPIRE].

[63] P. Agostini, T. Altinoluk and N. Armesto, *Non-eikonal corrections to multi-particle production in the color glass condensate*, *Eur. Phys. J.* **C 79** (2019) 600 [arXiv:1902.04483] [INSPIRE].

[64] G. Beuf, *Improving the kinematics for low-x QCD evolution equations in coordinate space*, *Phys. Rev.* **D 89** (2014) 074039 [arXiv:1401.0313] [INSPIRE].

[65] E. Iancu, J.D. Madrigal, A.H. Mueller, G. Soyez and D.N. Triantafyllopoulos, *Resumming double logarithms in the QCD evolution of color dipoles*, *Phys. Lett.* **B 744** (2015) 293 [arXiv:1502.05642] [INSPIRE].

[66] E. Iancu, J.D. Madrigal, A.H. Mueller, G. Soyez and D.N. Triantafyllopoulos, *Collinearly-improved BK evolution meets the HERA data*, *Phys. Lett.* **B 750** (2015) 643 [arXiv:1507.03651] [INSPIRE].

[67] Y. Hatta and E. Iancu, *Collinearly improved JIMWLK evolution in Langevin form*, *JHEP* **08** (2016) 083 [arXiv:1606.03269] [INSPIRE].

JHEP10(2019)208